Mortar Analyses of 12^{th}-18^{th} Century Buildings along the Belgian and Southern Dutch Coast.

Judith J. Mulder

September 22, 2011

Master's Thesis Archaeometry

Course code: 450300

ECTS: 27

Student number: 1473883

Responsible lecturer: Henk Kars

Daily supervisor: Adriaan de Kraker

Abstract

Mortars from 12^{th} to 18^{th} century buildings along the Belgian and southern Dutch coast have been analysed macroscopically, microscopically and by using TGA and FT-IR. The aim of these analyses has been to determine whether the location, date and initiators of the buildings (Cistercian or non-Cistercian) had influence on the composition of the mortar.

Macroscopy resulted in fourteen groups based on colour and thirteen groups based on the presence of certain grains. Two groups and two subgroups have been made using microscopy, five groups using TGA and six groups using FT-IR. When two samples appeared in the same group when they were analysed using one method, they were often not in the same group when analysed using a different method.

Groups based on TGA results correspond in terms of location, and groups made of microscopy and FT-IR relate only partly. The samples of only one of the buildings show a link between the composition of the mortar and the date. No relation was found between the composition of the mortar and the building owner, except for small differences in the presence of grains which were noticed during the macroscopic analyses.

The angular grains found during the microscopical analyses indicate that the quartz sand came from rivers. The source of the lime could not be determined, but regarding the distance, it would be most logical that it came from shells.

In conclusion, we can establish that local material was most probably used for the mortar.

Figure front page: mortar of the 'Hof te Zande' church, Kloosterzande (the Netherlands) (taken by the author).

Contents

Chapter 1

Introduction

1.1 Framework of the project

The Order of Cîteaux was founded by Robert of Molesme in the south of Dijon in the east of France in 1098 and was established because a group of monks chose to follow the Rule of Benedictus more strictly than was possible in other abbeys (Verbaal, 2005). This Rule was the basis of the life in European abbeys from the first half of the sixth century onwards (De Bleeckere, 2005).

Five abbeys were a member of the Order in 1115, among which Clairvaux. The Order of Cîteaux grew to more than 280 members while Bernardus was abbot of Clairvaux, until his death in 1153 (Vanderputten, 2005). During the 12^{th} and 13^{th} centuries, the Order extended as far as Portugal, Ireland, Norway, Estland and Syria (Kinder, 2002).

The planning of a new abbey required either a monk with experience in building (Lloyd, 2006), a monk who was a master builder (Sease and Schmidt-Brabant, 2007) or a consultant (Delaey, 2005), who was sent from an older abbey. Alternatively, a professional master builder who traveled from project to project could be employed instead of a monk, as well as professional builders with various specialties (e.g. quarrymen, masons) (Moffett et al., 2003).

Although no detailed specifications or guidelines existed about the shape of the buildings, the Cistercians (the people from the Order of Cîteaux) followed the design that had been used for many abbeys since the 9^{th} century onwards. The fact that almost all Cistercian abbeys were built according to the same plan may have resulted from the rapid growth of the monastic community and also because monks were sent from the main abbey to the subsidiary abbeys for construction and providing or advice. In contrary to the abbeys themselves, the secondary and farm buildings differed at various locations (Delaey, 2005).

This thesis comprehends the study of buildings from six sites, three Cistercian and three others. The buildings on the Cistercian sites are all secondary buildings related to the Cistercian Abbey of Our Lady of the Dunes ('Ten Duinen' Abbey) in Koksijde (Belgium). It is unknown whether these were actually built by monks. This is examined by studying the differences in the mortar used in buildings from Cistercian clients compared with buildings commissioned by other clients. This and differences in location and date are studied by analysing various mortars.

This thesis has been written for my Master's Thesis Archaeometry, which is part of the Master's programme of Earth Science, specialisation Archaeometry, at the VU University Amsterdam. I aim to achieve greater knowledge of Medieval building styles, the methods of building and use of materials.

1.2 Reading guide

This chapter has given an introduction to this thesis. *Chapter 2* outlines the definition of the problem (including the research questions) and the background information (including the historical background, mortar and previous research). *Chapter 3* presents the samples taken for analyses, including the locations of these samples. The methods used are described in *chapter 4*. The results are described and grouped in *chapter 5*. The data set is discussed in *chapter 6*. This is a study of the possible existence of a link between the groups made in chapter five and the location, date and owner of the buildings. Furthermore, the results of the different methods are compared. Finally, *chapter 7* contains the conclusion, including what can be done in further research. This is followed by the *acknowledgements* and *references*.

Chapter 2

Definition of the problem and background information

2.1 Definition of the problem

The main *research question* I aim to answer in this research is:

- *Do the location, date and building owner have influence on the composition of the mortar?*

Therefore, the following sub questions need to be answered:

- *Do mortars show differences in terms of location, period and building owner?*
  - *What is the composition of the sampled mortars?*
    - *What is the provenance of the material? Does the lime from the mortar come from shells or from limestone?*
  - *What groups of building styles can be made based on the composition of these samples?*

I hope to answer these questions in this thesis by measuring the samples taken from various locations in western Belgium and the south-western Netherlands.

Hypotheses:

I assume that the mortars contain much lime. The six locations are all near the coast where shells and quartz sand, which can be used for making mortar, are available, so probably local material was used.

I expect the mortar of the buildings to be quite the same. Since the people who built the buildings had connections with each other (as they lived in the same area or they had the same initiator), they might have had the same methods of building and preparing of mortar. However, there may be some differences, because of the distance between the locations and probably because local material was used.

I think that location has the largest influence on the mortar, since I expect that local material is used, regardless the period. It is unknown whether a difference exists between the Cistercian and the other buildings. When the Cistercian buildings are built by monks, they might differ from the other buildings, but they might as well be built by the same people as the other buildings.

2.2 Historical background and study area

The locations that have been chosen to study are all related to the abbey 'Ten Duinen' in Koksijde (Belgium). Some are located nearby the abbey and some are historically related. Unfortunately, no reliable samples could be taken from the abbey 'Ten Duinen', since its remains have been excavated and intensely restored without proper documentation (Dewilde and De Meulemeester, 2005).

The abbey 'Ten Duinen' was founded in 1128 and joined the Order of Cistercians in 1138 (Devliegher, 1954). The building was rebuilt out of brick in the 13^{th} century, since the community grew (Dewilde and De Meulemeester, 2005).

Hence also the subsidiary abbey 'Ter Doest' at Lissewege (D in fig. 2.1) was founded in 1175 (Delaey, 2008). As more people joined the abbey, 'Ten Duinen' needed more farmland. It started to cultivate, reclaim and embank land, for example in Zeeuws-Vlaanderen, which was granted by the Flemish counts. Consequently, 'Hof te Zande' was built at Kloosterzande (Z in fig. 2.1) in the 13^{th} century (Fruytier, 1950).

In the Eighty Years' War, the monks fled from 'Ten Duinen'. Between 1578 and 1584, the protestant government of Veurne ordered to remove 'Ten Duinen'. In 1601, the monks regrouped at 'Ten Bogaerde' (B in fig. 2.1) at which already buildings of the community were located (Van Royen, 2005), among which a barn from the 13^{th} century which still exists (Lehouck, 2008). New buildings were built and older ones were restored. In 1627, the most monks moved to Brugge, while a few stayed at 'Ten Bogaerde' (Van Royen, 2005).

To compare the mortar of these Cistercian buildings with non-Cistercian buildings, the following buildings were also studied. Some samples have been taken from excavated bricks of the church of the drowned village of Aendijcke (A in fig. 2.1), since this church and the church of 'Hof te Zande' are at close range and existed at the same time. The church at Wulveringem, nearby Koksijde and Veurne, (W in fig. 2.1) was sampled since it still contained some 12^{th} century material (Firmin, 1940). In addition, various samples were taken from buildings in the city Veurne (V in fig. 2.1) which is nearby 'Ten Duinen'.

Figure 2.1: Overview of the sample locations (Based on `http://maps.google.com`, 2010 and Google Earth).
A: Aendijcke (The Netherlands) V: Veurne (Belgium)
B: 'Ten Bogaerde', Koksijde (Belgium) W: Wulveringem (Belgium)
D: 'Ter Doest', Lissewege (Belgium) Z: 'Hof te Zande', Kloosterzande (The Netherlands)

2.3 Mortar

Mortar is studied in this thesis since it is expected that different building phases can be distinguished by studying Medieval mortar, as was done by studying Roman mortars in various studies (see 2.4).

2.3.1 Production process and composition

Mortar exists of binder (lime in most periods), aggregates (often sand) and sometimes aiding materials (Van Balen, 2003). These three groups are described below.

Binder is the component that binds the aggregates and the bricks of the building when it hardens (Van Balen, 2003; Durbin, 2005). Clay and calcium carbonate were used as binder in the Middle Ages. Calcium carbonate is obtained from limestone or shells and heated until a temperature of 900°C (Van Balen, 2003):

$$CaCO_3 \text{ (calcium carbonate)} \rightarrow CaO \text{ (quicklime)} + CO_2 \text{ (}\uparrow \text{ gas)}$$

The quicklime is quenched with water to form slaked lime (Van Balen, 2003):

$$CaO \text{ (quicklime)} + H_2O \text{ (water)} \rightarrow Ca(OH)_2 \text{ (slaked lime)}$$

The slaked lime reacts with CO_2 from the air whereby calcium carbonate is formed again. The lime hardens in this phase (Van Balen, 2003):

$$Ca(OH)_2 \text{ (slaked lime)} + CO_2 \rightarrow CaCO_3 \text{ (calcium carbonate)} + H_2O$$

This reaction is the short version of the two sub reactions that take place (Van Balen, 2003):

$$\text{a) } CO_2 + H_2O \rightarrow H_2CO_3$$

$$\text{b) } Ca(OH)_2 + H_2CO_3 \rightarrow CaCO_3 + 2\ H_2O$$

Aggregates are added to the slacked lime (Goffer, 2007) to prevent shrinking of the mortar when it hardens (Van Balen, 2003). Sand is the most used aggregate, others are broken shells, slags, pieces of coal and hair.

Aiding materials (pozzolans) are added in order to enhance the hardening (increase the hydraulicity, see 2.3.2) and final strength of the lime mortar. Materials that can be used as pozzolanas are for example baked clay and powder from milled stones, for example trass (milled tuff) (Van Balen, 2003).

2.3.2 Mortar types

Mortar has been used for a long time. The first known mortar was made from loam and flattened soil. It was found in Çatal H*üyük* and dated at 6000 BC (Van Balen, 2003). The Egyptians used mortar made from burned gypsum and sand from the third millennium BC onwards (Kreh, 2002). Lime was first used as plaster in Greece from the 6^{th} century BC onward. Lime mortar was first used at the end of the second or the beginning of the first century BC in Greece, after which it was used widely by the Romans which often added puzzolana and milled ceramics which increase the hydraulicity (Van Balen, 2003).

The hydraulicity depends on the purity of the material. Non-hydraulic lime exist of pure lime ($Ca(OH)_2$), while hydraulic lime also contains calciumsilicates and oxides. Non-hydraulic lime hardens by air, while hydraulic lime can harden by a chemical reaction with water. It can harden under water without contact with air. This means that the entire amount hydraulic

lime can harden at the same time, while non-hydraulic lime starts hardening at the surface (Van Balen, 2003).

In the Middle Ages, raw materials had to be obtained from nearby the building site, since transport over large distance was too expensive. This caused many differences in composition between different locations (Van Balen, 2003).

Lime mortar was used until Portland cement was introduced by the end of the 19^{th} century. This is modern material consisting of tricalciumsilicates which hardens very fast, even faster than hydraulic lime which consists of dicalciumsilicates (Van Balen, 2003).

2.4 Previous Research

Various research has been done on mortar. The hydraulicity appears to be one of the most important factors to find differences in mortars of historic buildings (Van Balen, 2003). Hydraulicity research has successfully been done in various studies (e.g. Kootker, 2007a, b; Moropoulou et al., 2003) using Thermogravimetric analysis (TGA). Moropoulou et al. (2003) could successfully group mortar in four categories based on TGA analysis. Kootker (2007b) could make two groups of her mortars.

The presence of components as calcite, quartz, portlandite, brucite, K-feldspars (Biscontin et al., 2002) and iron oxides (Genestar et al., 2006) has been indicated using Fourier transform infrared spectroscopy (FT-IR).

The methods TGA and FT-IR (which measures which compounds are present) are often applied on the binder, for which the <63 μm fraction is mostly taken (e.g. Biscontin et al., 2002; Genestar et al., 2006; Kootker, 2007b). Sometimes another fraction is taken (<40 μm in Silva et al., 2005).

Microscopy provided information about the aggregate content (Pavia et al., 2008), binder / aggregate ratio and grain size (Kootker, 2007 a and b).

Other methods that are sometimes applied are for example Granulometric analysis (e.g. Maravelaki-Kalaitzaki et al., 2003; Kootker, 2007b), scanning electron microscopy (SEM) (e.g. Moropoulou et al., 2000; Silva et al., 2005), X-ray diffraction (XRD) (e.g. Genestar et al., 2006), and X-ray fluorescence (XRF) (e.g. Velosa et al., 2007).

Not enough time was available to use all these methods in this research, so only microscopy, FT-IR and TGA were chosen, since they are often applied in previous research and were considered to be the most useful. Granulometric analysis is not very reliable for measuring the binder/aggregate ratio, since brittle aggregates can be present in the material, such as ceramics and some stones, which can break into fine material (Maravelaki-Kalaitzaki et al., 2003) and binder can be cohere to larger aggregates (Kootker, 2007b). Aggregates, such as mica, plagioclase and pyroxene have been identified using SEM (Silva et al., 2005) and pore size distribution has been studied (Moropoulou et al., 2000). An optical microscope was used instead of SEM, since it can also study the aggregates and pores and it is easier to use and to obtain. XRD only showed the presence of calcite and quartz in some studies (Genestar et al., 2006; Kootker, 2007b), so no additional information was provided to the TGA and FT-IR results. However, XRD has identified other material like muscovite, gypsum, plagioclase in an other study (Maravelaki-Kalaitzaki et al., 2003). XRF could have been useful, since it can measure various components in the sample, e.g SiO_2, CaO, Al_2O_3, Fe_2O_3 (Velosa et al., 2007), but it does not add much information if FT-IR is already used.

Most studies are done on sites from the Mediterranean, for example in Portugal (e.g. Velosa et al., 2007), Spain (e.g. Genestar et al., 2006), Italy (e.g. Silva et al., 2005) and Greece (e.g. Moropoulou et al., 2000). The studied buildings are often from the Roman period. Since the location and period is different, the mortar might have been produced differently too, using

different ingredients. Degradation may also differ.

Mortar from sites in Belgium is also studied. Macro-, optical microscopy and polarisation fluorescence microscopy were applied on lime mortar from the cathedral of Tournai. The aggregates and binder types were identified and binder/aggregate ratio, grain sizes and degradation were studied. Differences in composition between building periods were found (Elsen, 2006; Mertens et al., 2009). Leysen et al. (1990) studied various samples from sites throughout Belgium using electron probe X-ray micro-analysis, petrographical and electron microscopy, X-ray fluorescence, ion chromatography and atomic absorption spectrometry. Differences in composition were found between the underlying material and crust which indicate weathering and pollution.

I think this research, in which I study mortar from sites in Belgium and the southern Netherlands using macro- and microscopy, FT-IR and TGA, can contribute to the understanding of mortar in general.

Chapter 3

Sample locations

A total of 48 samples was taken from six locations, representing 3 structures or buildings in the Netherlands and 14 in Belgium. Three of the six locations contain more than one building. The sample locations are described below and maps and/or pictures of the buildings are included. If not stated otherwise, the pictures are taken by the author.

3.1 Hof te Zande

The church and the nearby wall (fig. 3.1) of 'Hof te Zande' at Kloosterzande (Zeeuws-Vlaanderen, The Netherlands) have been studied.

The church was built at the beginning of the 13^{th} century (DeVlieger, 1954; Stichting de Kerk in Klooster, 2009). It was largely destroyed during the Eighty Year's War at the end of the 16^{th} century, and rebuilt in 1609 (Fruytier, 1950; De Kraker, 1997). It was restored between 1922 and 1924 (Stichting de Kerk in Klooster, 2009). The shape stayed the same, since it was rebuilt according to the original plan of the 13^{th} century (personal communication P. Overduin and C. Crans, 2010). According to Vincent Debonne (personal communication, 2010), researcher of architectural heritage, the 13^{th} century construction phase is still present at the eastern and south-eastern wall. The rest is from the 17^{th} or 20^{th} century.

Ten samples were taken (fig. 3.2 and table 3.1). The samples that have been taken from the eastern wall (1 and 2), the southern wall east of the extension (4 and 5) and the well (6) are medieval (13^{th} century) (personal communication V. Debonne, 2010 and P. Overduin, 2010). Sample 7 is modern, probably from 1922. The other samples are from the rebuilding phase of 1609.

The area of 'Hof te Zande' was surrounded by walls and deep ditches under abbot Theodoricus (1259-65') (Fruytier, 1950). A part of that wall is still present and sampled for this research. The wall is built out of medieval bricks, but it is not known whether it is original or if the bricks have been reused. Also 17^{th} century bricks are present in some parts of the wall (Scez, 2010). The age of the wall is not very reliable, since the wall is often repaired and rebuild.

The wall exists of flat sides with buttresses between them (fig. 3.3(h)). There are 13 flat sides at the larger part of the wall and 5 at the smaller. The flat sides are about 210 cm long. The vertical structures are about 40 cm wide and stick out about 7 cm. Some flat sides exist only of the smaller 17^{th} century bricks (e.g. flat side 3) and some of smaller (17^{th} c.) and larger (medieval) bricks (e.g. flat side 8, fig. 3.3(i)). All samples have been taken from the northern side of the wall. They are described in table 3.1.

Since sample 1, 2 and 3 are taken from mortar near the smaller bricks, the mortar has to be from the 17^{th} century or younger. Sample 4 is taken from mortar near larger bricks, so might

be medieval (13^{th} century), but this part of the wall may also be rebuilt in the 17^{th} century or later.

Figure 3.1: 'Hof ter Zande', view from the west. The wall is visible at the right.

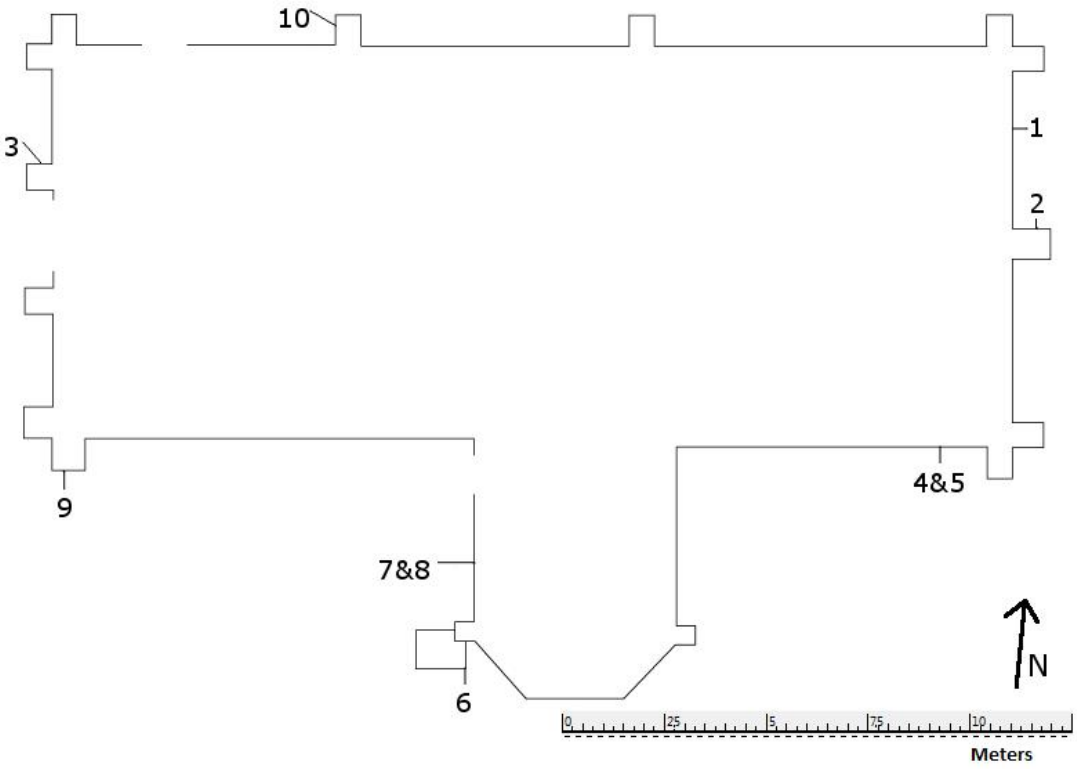

Figure 3.2: 'Hof ter Zande', map of the church with sample locations.

Figure 3.3: Sample locations at 'Hof te Zande'.
First row left (a): Zc.1 and Zc.2 (©N. de Kraker). Right (b): Zc.3.
Second row left (c): Zc.4 and Zc.5 (©N. de Kraker). Right (d): Zc.6.
Third row left (e): Zc.7 and Zc.8 (©N. de Kraker). Middle (f): Zc.9. Right (g): Zc.10.
Fourth row left (h): The wall including the flat sides and buttresses, the third flat side is in the middle of the picture. Right (i): The eight flat side, the white circle indicates the location of sample Zw.3.

Sample	Wall	Location	Height (cm)	Photo 3.3	Date
Zc.1	Eastern	134 cm from the buttress at the north.	137	a	13^{th} c.
Zc.2	Eastern	At the northern side of the middle buttress. 62 cm from the wall to the west.	183	a	13^{th} c.
Zc.3	Western	At the northern side of the buttress left of the door. 20 cm from the wall at the east.	9	b	1609
Zc.4	Southern	Right from the extension, 90 cm from the buttress at the east.	133	c	13^{th} c.
Zc.5	”	Same as Zc.4, but deeper into the wall.	”	c	13^{th} c.
Zc.6	Well	Southwestern corner.		d	13^{th} c.
Zc.7	Western wall of the extension at the south.	143 cm from the buttress at the south and 306 cm from the wall to the north.	101	e	1922
Zc.8	”	Same as Zc.7, but deeper into the wall.	”	e	1609
Zc.9	Southern	30 cm from the end of this buttress at the west.	130	f	1609
Zc.10	Northern	Second buttress from the west. 33 cm from the end of this part at the north.	144	g	1609
Zw.1	3th flat side from the east	170 cm from the eastern buttress.	127	h	17^{th} c. or later
Zw.2	8th flat side from the east	105 cm from the eastern buttress.	88	i	17^{th} c. or later
Zw.3	8th flat side from the east	At about 1/3 from the part from the western buttress.	4th-5th brick row from the top	i	17^{th} c. or later
Zw.4	Buttress between 12th and 13th flat side from the east.	Entire wide.	114	-	13^{th} c. or later

Table 3.1: Locations and dates of the samples from the church (Zc) and nearby wall (Zw).

3.2 Aendijcke

The Medieval village of Aendijcke was flooded in 1584 (De Kraker, 1997) and it was located at the recent hamlet Poonhaven (Zeeuw-Vlaanderen, The Netherlands). It is unknown when this church was exactly built, probably in the 14^{th} or 15^{th} century (personal communication A. de Kraker, 2011). An excavation took place in the flooded village Aendijcke in 1980 at which the remains of a church were found. The mortars of two bricks of that church (table 3.2) are analysed in this research. The oldest known visual information about the church is a map of Franchoys Horenbault from 1569 (fig. 3.4), so the mortar is certainly from before this date.

Sample	Location	Date
A.1	At a brick of 29x14x8 cm.	Before 1569
A.2	At a brick of 28x13x7 cm.	Before 1569

Table 3.2: Location and date of the samples from Aendijcke (A).

3.3 Ter Doest

The only building remaining from the Medieval abbey ‘Ter Doest’ is a barn (fig. 3.5 left). This barn has been dated with dendrochronology at about 1375, while its masonry has been dated at the 13th century (Delaey, 2008).

Samples (table 3.3) could be taken at only one location of the Medieval barn of abbey ‘Ter Doest’. This was at the inside, at the northern wall, behind the most north-western wooden pillar (fig. 3.5 right). A hole was already present in the wall at that location. The rest of the walls were very hard and were painted white. A drill was needed for the other walls, but that

was not available. The age of the eastern and western walls (the long sides) could not be trusted (personal communication B. Delaey, 2010).

Figure 3.4: Aendijcke. Horenbault, 1569. No. 2647 in Maps and plans, State Archives, Gent, Belgium.

Figure 3.5: $13^{th}/14^{th}$ century barn of the abbey 'Ter Doest', Lissewege. Left: Overview picture. Right: Sample location at the most north-western wooden pillar.

3.4 Ten Bogaerde

A 13^{th} century (Lehouck, 2008) barn (fig. 3.6 upper left) is located at 'Ten Bogaerde' which belonged to the 'Ten Duinen' abbey. Four samples have been taken from what used to be the inside of the north-eastern wall (fig. 3.6 upper right and bottom). Nowadays, the north-western wall has been torn down and a new wall is built in the middle of the old barn, leading to a smaller barn.

The abbot's house (fig. 3.7 upper left), which was finished in 1612 (numbers on the wall;

Sample	Location	Date
D.1	Inside of the barn, near the north-wester wooden pillar, 104 cm above the surface, 20 cm deep into the wall.	13^{th}-14^{th} c.
D.2	Same as D.1, but 24 cm deep into the wall.	13^{th}-14^{th} c.

Table 3.3: The location and date of the samples from Ter Doest (D).

Lehouck, 2008) was built when the monks from 'Ten Duinen' regrouped at 'Ten Bogaerde' during the Eighty Years' War. Three samples have been taken from this house (fig 3.7 upper right and bottom).

In addition, an 18^{th} century barn (fig. 3.8 upper left) is located at 'Ten Bogaerde' at which six building phases have been distinguished. The major part was built in 1742-1744. Only the wall at the southeast corner is dated older, probably 1597/1601-1627. Restoration works took place in the 19^{th} century, 1918-1949, 1949-1951 and after 1952, mostly along the windows and doors (Lehouck, 2010).

Samples 1 and 2 are from the part of the building that was built between 1742 and 1744 (fig. 3.8 lower left). Samples 3, 4 and 5 have been taken from the part of the building that is dated 1597-1627 (fig. 3.8 lower right). Sample 5 is more reliable than sample 4, because it has been taken from deeper into the wall. All joints at the outside were reflushed in the 1950's.

Table 3.4 presents the descriptions from the samples from 'Ten Bogaerde'.

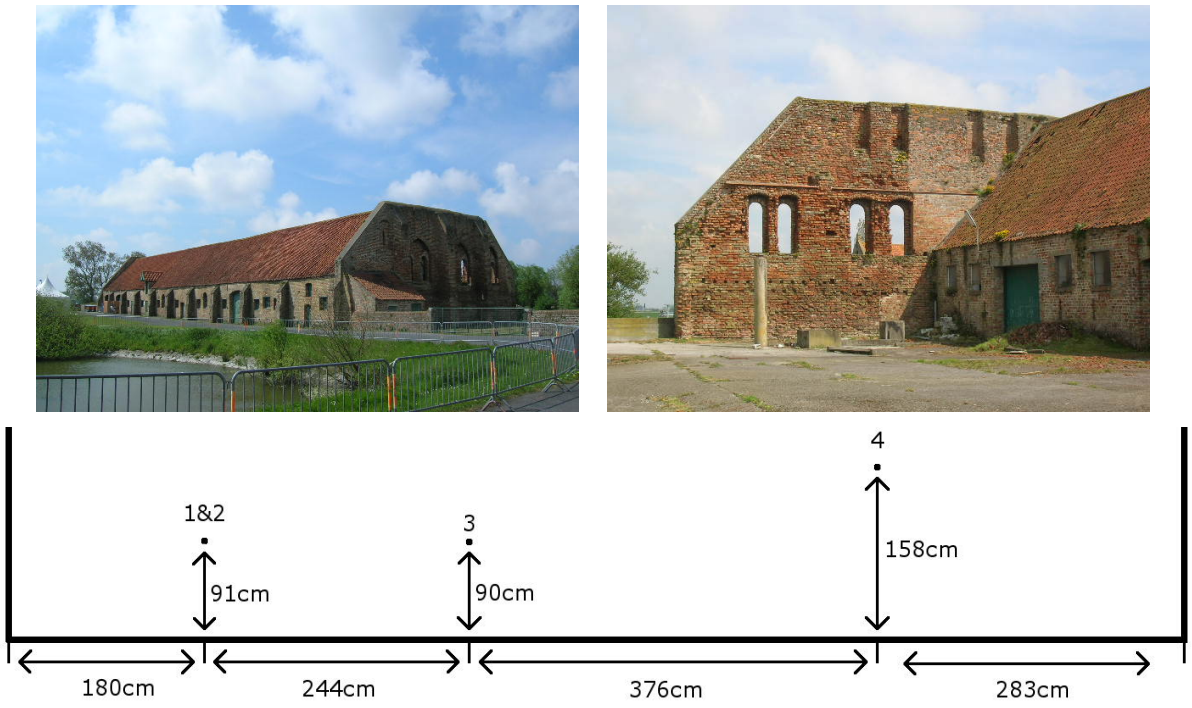

Figure 3.6: 13^{th} century barn of abbey 'Ten Bogaerde', Koksijde. Upper left: Overview photo. Upper right: The north-eastern wall seen from the west. Bottom: Schematic drawing of the bottom part of the north-eastern wall seen from the south-west, with sample locations.

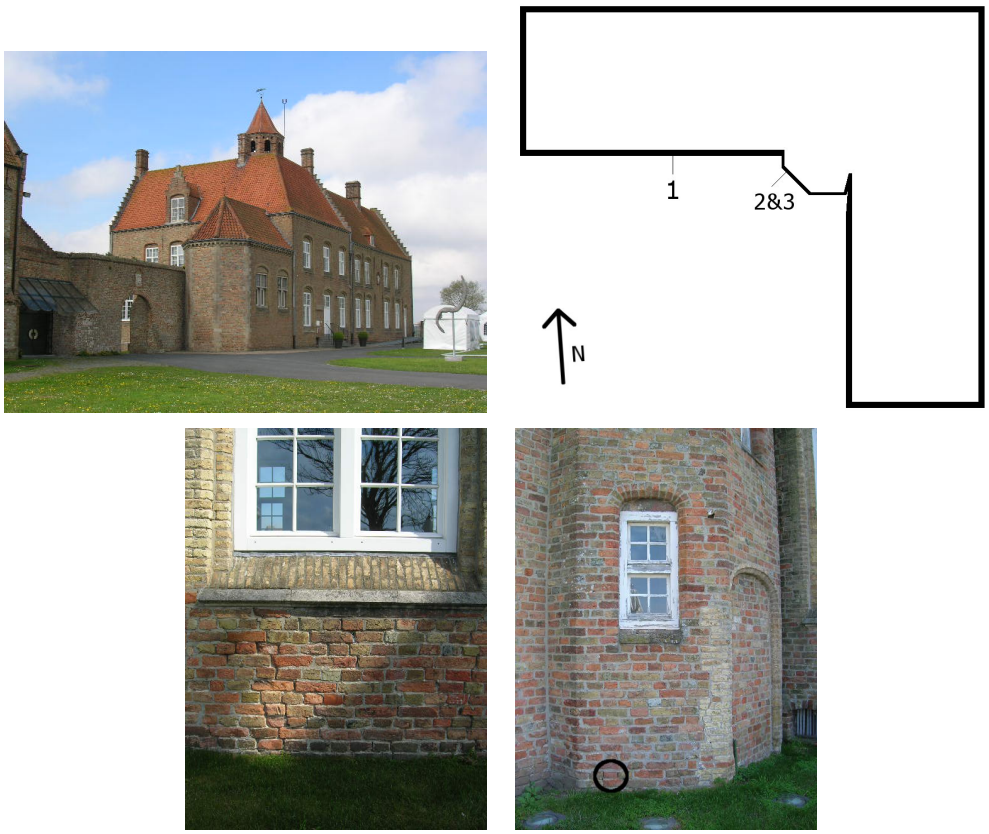

Figure 3.7: 17^{th} century abbot's house at 'Ten Bogaerde', Koksijde. Upper left: Overview photo. Upper right: Map of the abbot's house with the sample locations. Lower left: Sample location of Bb.1. Lower right: Sample location of Bb.2 and Bb.3.

Sample	Location	Height (cm)	Date
Ba.1	180 cm from the end of the wall at the left.	91	13^{th} c.
Ba.2	Same as Ba.1, but deeper into the wall, until 12 cm.	"	13^{th} c.
Ba.3	424 cm from the end of the wall at the left.	90	13^{th} c.
Ba.4	8 m from the end of the wall at the left.	158	13^{th} c.
Bb.1	Below the middle window in the southern wall. 45 cm from the right side of the window, which is 118 cm.	56	1602-1612
Bb.2	South-western side of the tower. 30 cm from the edge at the left.	8	1602-1612
Bb.3	Same as sample 2, but deeper into the wall.	"	1602-1612
Bc.1	Inside of the eastern side of the northern wall, at a bricked hole, probably a former window. The sample is taken at the corner right of the niche. 156 cm from the east wall.	166	1742-1744
Bc.2	14 cm from the left corner of the niche.	145	1742-1744
Bc.3	Outside, at the south-eastern corner. 35 cm from the end of the wall at the south.	150	1597/1601-1627
Bc.4	Near sample Bc.3, 29 cm from the end of the wall at the south.	140	1597/1601-1627
Bc.5	Same as Bc.4, but deeper into the wall.	"	1597/1601-1627

Table 3.4: Locations and dates of the samples from the Medieval barn (Ba), Abbot's house (Bb) and 18^{th} century barn (Bc) of 'Ten Bogaerde'.

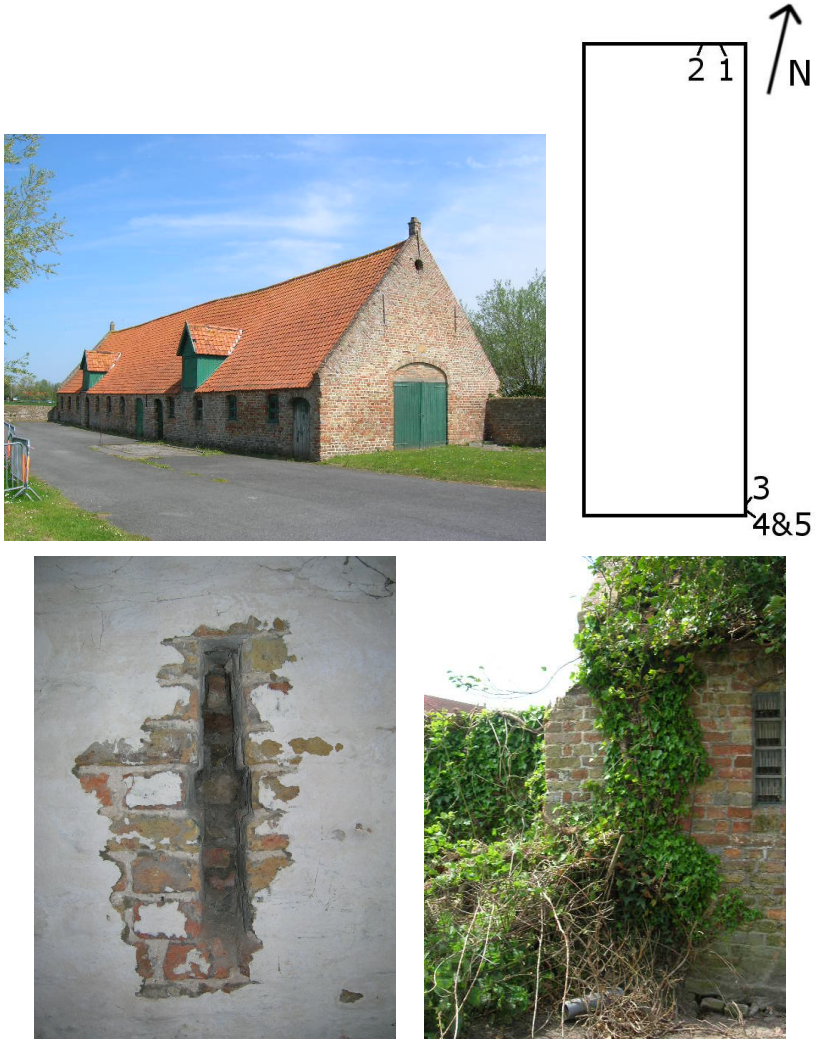

Figure 3.8: 18^{th} century barn at 'Ten Bogaerde', Koksijde. Upper left: Overview photo. Upper right: Schematic overview of the sample locations. Lower left: The niche at the northern wall. Lower right: The older part of the south-eastern corner of the building. The samples are taken left of the ivy.

3.5 Veurne

The city of Veurne is at least as old as the 7^{th}th century (Firmin, 1940) and many old Medieval buildings are still present which were available for sampling. Figure 3.9 shows an overview of all sample locations in Veurne.

One sample has been taken from the church of St. Walburga (fig. 3.10), which was built between 1213 and the beginning of the 14^{th} century (Lehouck, 2008). It replaced a Romanesque church of which parts were still standing until the beginning of the 20^{th} century (Firmin, 1940). The sample has been taken from south-eastern side of the choir, which was built in the first half of the 13^{th} century (Lehouck, 2008).

One sample has been taken from the St. Niklaas church tower (fig. 3.11), which was built in the 13^{th} century (Lehouck, 2008).

Three samples have been taken from the front of the 16^{th} century (Lehouck, 2002) school building at Noordstraat 21 (fig. 3.12).

In addition, samples from 6 buildings were provided by Alexander Lehouck, who took these for an earlier study (Lehouck, 2001). The Spanish Pavilion is a former town hall of which the oldest part was built in the period 1445-1447. The vault was made in 1492-1493 and an extension was built in the 16^{th} century (Lehouck, 2008). The sample was taken from the vault, so is from 1492-1493.

Table 3.5 shows the descriptions of the samples taken in Veurne.

Figure 3.9: Overview of the sample locations in the city Veurne (based on Google Earth).

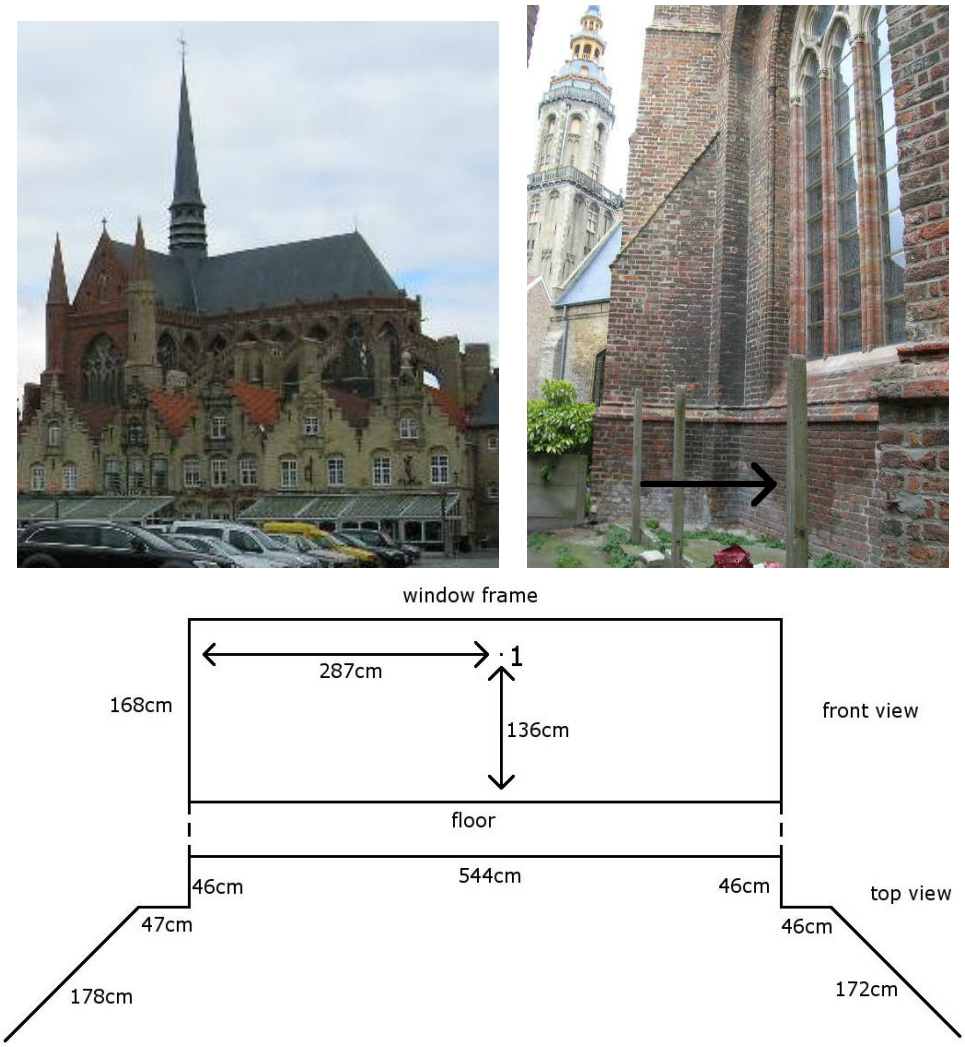

Figure 3.10: The 13^{th} century church St. Walburga, Veurne. Upper left: Overview photo. Upper right: Photo of the sample location. Bottom: Schematic overview of the sample location.

Figure 3.11: The 13^{th} century church of St. Niklaas, Veurne. Left: The tower. Right: The portal at the bottom of the tower with an arrow indicating the sample location.

Figure 3.12: 16^{th} century school, Veurne. Top: Overview photo. Bottom: Schematic overview of the sample locations.

Sample	Building	Location	Height (cm)	Date
Vb.1	Boterweegschaal-straat 3	Arch in the northern wall.	-	13^{th}-16^{th} c. (Lehouck, 2001).
Vb.2	”	Vault	-	”
Vg.1	Grote markt 16	-	-	16^{th} c.-first half of 17^{th} c. (Lehouck, 2001)
Va.1	Noordstraat 5	-	-	15^{th}-17^{th} c. (Lehouck, 2001)
Vc.1	Noordstraat 21	242.5 cm from the door to the right and 408 cm from the building to the left. Until 1 cm deep into the wall.	69	16^{th} c.
Vc.2	”	Same as Vc.1, but 1-9 cm deep into the wall.	-	”
Vc.3	”	319.5 cm from the door to the right and 331 cm from the building to the left.	63	”
Vd.1	Noordstraat 59	-	-	13^{th} c. (Lehouck, 2001)
Vo.1	Ooststraat 18	-	-	17^{th}-18^{th} c. (personal communication A. Lehouck, 2011)
Vn.1	St. Niklaas	22 cm left of the portal	29	13^{th} c.
Vs.1	Sp. Pavilion	Vault	-	short after 1492
Vw.1	St. Walburga	South-eastern side, at a wall below a window. 287 cm from the left of the part of the wall that is indicated in fig. 3.10(c).	136	13^{th} c.

Table 3.5: Codes and dates of the samples from buildings in Veurne (V).

3.6 Wulveringem

The Romanesque part of the ‘Onze Lieve Vrouwe Kerk’ in Wulveringem (fig. 3.13 left) has been built out of ironstone from the 12^{th} century onwards until the 14^{th} century. The church was rebuilt out of brick in the 16^{th} century. The last rebuilding took place in 1553 (Firmin, 1940).

Figure 3.13: 12^{th}-16^{th} century church, Wulveringem. Left: Overview photo (http://nl.wikipedia.org). Right: Sample 2 is taken at the part of the pillar at the right which is made of ironsandstone.

Samples have been taken at the inside and the outside of the church, the exact locations can be seen on the map (fig. 3.15).

Samples 1, 3, 4 and 5 have been taken from the northern columns of the 12^{th} century aisle which nowadays is the northern wall (Firmin, 1940) (fig: 3.14 left and middle). Sample 2 has been taken from a 12^{th} century column in the middle of the church (fig. 3.13 right), while sample 6 has been taken from a 16^{th} century window frame (fig. 3.14 right).

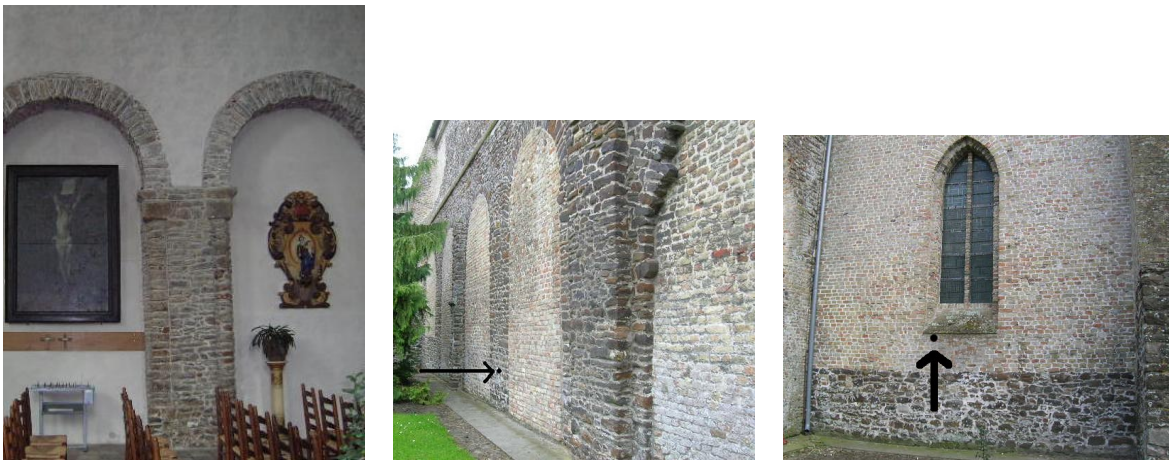

Figure 3.14: Sample locations at Wulveringem. Left: W.3 (W.1 is at a similar pillar). Middle: W.4 and W.5. Right: W.6.

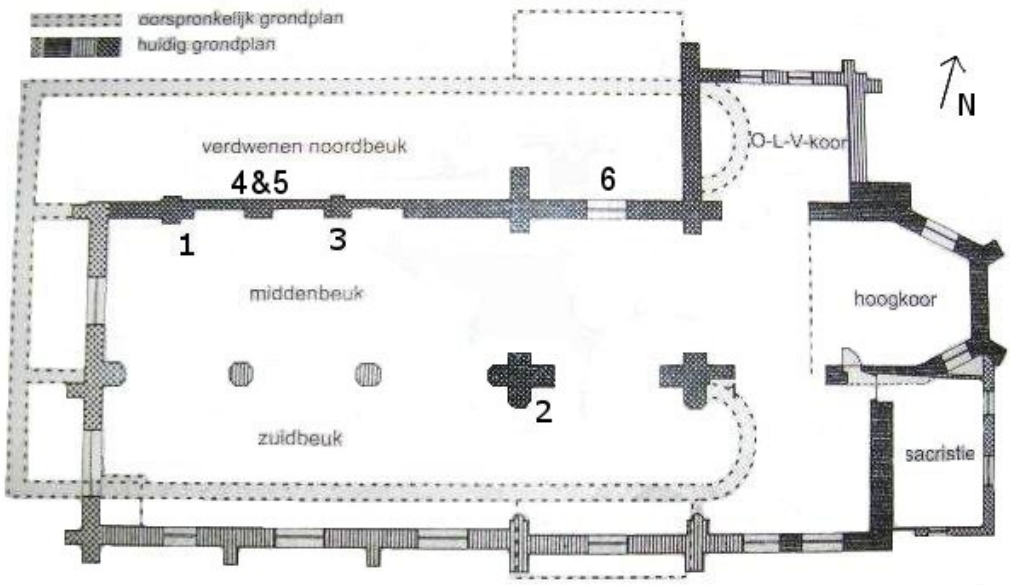

Figure 3.15: Map of the church of Wulveringem with the locations from which the samples are taken (based on a map found in the church).

Sample	Inside/ outside	Location	Height (cm)	Date
W.1	Inside	At the northern wall. About 70 cm from the wood at the right.	120	12^{th} c.
W.2	Inside	At the third pillar seen from the south-western wall of the church. At the ironsandstone part of the pillar, near the lighter brick part of the pillar.	90	12^{th} c.
W.3	Inside	At the northern wall. Between the second and third bow. The pillar between the two bows exists of rounded stones at the sides and flat stones in the middle. The third sample is taken 46 cm left from the border of the rounded and flat stones. The part of the flat stones was 59 cm in total.	138	12^{th} c.
W.4	Outside	This samples has been taken between the ironsandstones between the first and second bow seen from the south-west, that is 838 cm from the south-western side of the church.	60	12^{th} c.
W.5	Outside	At the same location as sample 2, but deeper into the wall.	”	12^{th} c.
W.6	Outside	This sample has been taken at the newer part of the church, just below a Gothic window, as a comparison. The location of the sample 167 cm from a wall to the left.	161	16^{th} c.

Table 3.6: Locations and dates of the samples from the church of Wulveringem (W).

Chapter 4

Methods

4.1 Sampling

A mortar sample of about 7 cm was needed for thin section, TGA and FT-IR. The samples have been taken with a hammer and chisel. Some samples were so loose that only a chisel was needed. The samples were put into plastic bags. The sample locations are described in chapter 3. Unfortunately, only loose material could be taken at most locations, so thin sections could be made of only 16 samples. FT-IR and TGA analyses have been done at 47 samples.

4.2 Macro- and microscopy

All samples have been macroscopically described. The colours of the dry material have been described using the Munsell colour chart after sampling. In addition, the grade of consolidation and the aggregate content have been noted.

Microscopical analyses have been done in order to describe the mineralogical composition of the samples and their texture. Not only the binder colour, the aggregate content and the amount, shape and size of the aggregates are studied, but also the amount and size of pores and an estimation of the binder/aggregate ratio are given. The thin sections are observed in PPL (Plane Polarized Light) and XPL (Crossed Polarized Light).

4.3 TGA

Thermogravimetric analysis (TGA) has been performed in order to distinguish different kinds of mortars. The hydraulicity index of the studied mortars was calculated using TGA, in order to distinguish hydraulic and non-hydraulic mortar. This has been done earlier, for example by Kootker (2007 a and b), Moropoulou et al. (2003) and Bakolas et al. (1998). Furthermore, the amount of $CaCO_3$ in the samples can be measured.

The principle is as follows. When samples are heated, the instrument measures weight loss as a function of temperature. Since certain materials burn or evaporate at certain temperatures, the loss of weight during a temperature range indicates which and how many material was present in the sample.

Only the <63 μm fraction of the samples has been measured with TGA. Besides that fine material is required for the methods, it is done since this fraction is considered as the binder, although also fine aggregates can be found (Moropoulou, 2000; Biscontin et al., 2002; Kootker, 2007b). Sand and larger aggregates are filtered out during the sieving, since sand has a grain

size ranging from 63 μm till 2mm. Only grains with the size of silt (4-16 μm) and clay (<4 μm) are present (Nichols, 2009). TGA (and FT-IR) measurements of this fraction were successfully done in previous research (e.g. Moropoulou, 2000; Biscontin et al., 2002; Kootker, 2007b).

Since the samples were difficult to sieve, they were dried in an oven, in order to remove some of the water, which caused the samples to stick together. The first group of samples was put in the oven for 4 days at 60°C, the second group was put in the oven for 5 days at 50°C. After the samples were heated, they were much easier to sieve.

Some samples were crushed before they were sieved, since they were more consolidated than the other samples. These samples are: A.1, A.2, Bc.4, Vg.1, , W.4, Zc.3, Zc.4, Zc.6, Zc.7, Zc.10, Zw.1, Zw.2, Zw.3, Zw.4. This was done using a crusher of the brand Janson. The crushing was done carefully, trying to avoid the aggregates.

The sieving was done using a mechanical sieve: Fritsen ®analysette Type: 03.502 No. 130 volt: 220. Two identical <63 μm sieves were used, of the brand Retsch®.

The instrument that is used for analysing is the TGA-701 analyzer from LECO Corporation. The samples are heated from 25 to 1000°C. Three temperature ranges at which certain material disappears are chosen to study:

120-200°C: weight loss due to disappearance of water chemically bound to hydrated salts.
200-600°C: weight loss due to disappearance of structurally bound water (SBW) bound to hydraulic compounds.
600-1000°C: weight loss due to disappearance of carbon dioxide during the decomposition of the carbonates.

The weight loss (%) between two temperatures can be calculated by the following formula, in which w(a) is the weight at the lowest temperature, while w(b) is the weight at the highest temperature and w(i) is the initial weight, measured at 105°C, after the moisture has been evaporated:

$$\frac{\text{w(a)} - \text{w(b)}}{\text{w(i)}} \times 100\% = \text{weight loss (\%)}$$

The hydraulicity is described by the CO_2/SBW ratio. This is the weight loss between 600 and 1000°C divided by the weight loss between 200 and 600°C.

The instrument also calculates the weight percentage $CaCO_3$ in the range 615-1000°C. This is calculated by using the following formula:

$$\frac{\text{w(615°C)} - \text{w(1000°C)}}{\text{w(150°C)}} \times \frac{10000}{44} = \text{weight loss (\%)}$$

$\frac{10000}{44}$ is used instead of 100, because the ratio between $CaCO_3$ and CO_2 is 100:44 in the equation that shows how the bonds of $CaCO_3$ break during heating:

$$CaCO_3 \rightarrow CaO + CO_2$$

The sample size differs from 0.2416 to 0.9212 grams. The sample size is sometimes very small, since only few sample was available.

4.4 FT-IR

Fourier transform infrared spectroscopy (FT-IR) can measure which bonds of atoms are present in a sample. The method is used because it can measure whether for example carbonate, silica, iron oxides and organic material are present (e.g. Kootker, 2007b).

As for TGA only the <63 μm fraction was measured, so the samples had to be sieved. Only fine material can be measured with FT-IR.

The principle

Two atoms connected by a chemical bond vibrate relative to each other. If one of these atoms is positive and the other is negative, there is an electric dipole moment. The frequency of the vibration (v) depends on the strength of the bond (k) and the weight of the atoms (m):

$$\mathrm{v} = \frac{1}{2\pi}\sqrt{\frac{\mathrm{k(m1 + m2)}}{\mathrm{m1 \times m2}}}$$

At FT-IR, infrared radiation is set to pass through the sample. When a photon collides to a bond, it will be absorbed, which causes the bond to vibrate more. The molecule can only absorb radiation with a frequency equal to the frequency at which the bond vibrates and only when there is a change in dipole moment.

The instrument measures the transmittance (%) corresponding to a wavenumber (cm^{-1}). Each wavenumber corresponds to a certain chemical bond. The wavenumber ($\widetilde{v}$) is the frequency of the vibration (v) divided by the speed of light (c: 2.998 $\times$ 10^8 m/s). The transmittance is the difference between the incoming and outgoing infrared radiation:

$$\mathrm{T} = \mathrm{I}/\mathrm{I}_0$$

A blanc has to be measured before the samples in order to determine I_0 and to be able to correct for the loss of radiation due to reflection (when light hits an object it reflects, transmits, or gets absorbed) and absorption by components in the atmosphere (H_2O, CO_2) (Ariese, 2010).

Testing submethods and analysing

Two FT-IR submethods were available: ATR (Attenuated Total Reflectance) and KBr (Potassium Bromide). In order to see which submethod was more suitable for this research, 3 samples were measured with both submethods and with different settings.

The KBr method was chosen, because much noise was visible at the ATR spectra, while the peaks of the KBr spectra were more clear. A resolution of 4 was chosen, because this causes the sharpest and so clearest peaks. Resolutions of 8 and 16 were also used at the test measurements, but this causes the peaks to flatten, so smaller peaks might not be visible. 16 scans were made at each measurements. The more scans the more precise the measurements are, but the longer the measurement takes. The range was 4000-400 cm^{-1}, which is the mid-infrared region (Harris, 2002), and the interval was 2.0. The unit on the y-axis was % T (Transmittance).

Blanc correction was applied on the measurements. Therefore, a pellet made of pure KBr was measured. This shows the background, for example the CO_2 and water vapor, which is also measured. The spectrum of this background measurement will be subtracted from all following measurements. In order to measure the samples, pellets were made by mixing and compressing 2 mg sample and 100 mg KBr.

Chapter 5

Results

5.1 Macroscopic description

All 48 samples are macroscopically described. An overview of these descriptions is shown in table 5.1.

The main distinctive property is colour. The samples are of different shades of gray and yellow. The Munsell system is used to describe the colours.

A distinction has also been made between samples existing of loose material and samples of which the material was cemented together. Small consolidated pieces are often present in loose material. This is not the consequence of the original composition, but of weathering.

Besides binder several other grains are present in the sample, such as chunks of lime and aggregates. The aggregates found during this research are bricks fragments, pieces of shells, (char)coal, rock and organic material. Some grains could not be identified. The white grains are probably lime or rock (e.g. quartz) and the red and orange grains are probably pieces of brick. Brown grains could be a piece of either brick or rock (e.g. flint, sandstone, mica) and a black grain can be a piece of either rock (e.g. mica) or (char)coal. A grey grain could be a piece of brick, rock or a dull piece of (char)coal.

If aggregates are not noted in the table, it does not necessarily mean that a sample does not contain that material. The aggregates may be very small and so not clearly visible. Microscopical analyses will give more detailed information.

5.1.1 Discussion and conclusion

Fourteen groups were made based on sample colour (table 5.2). Some samples have an unique colour, while seventeen or eighteen samples have the colour 7.5Y 8/1.

Groups can also be made based on the identifiable grains. In order to look for an overlap in identifiable grains at the samples, the amount of the occurrence of these grains is noted: 15 of the 48 samples contain brick, 37 contain lime, of which 4 shells. 4 samples contain (char)coal and 8 possibly. 9 contain grey rocks, 3 samples contain some kind of organic material, of which one contains wood.

Then it is noted how many times a certain combination of identifiable grains occurs. Since the presence of five grains is noted, 32 (2^5) combinations can be made. Table 5.3 shows no clear relation between the presence of various grains. Fourteen out of 32 combinations occur at these samples. Some combinations are only shown at one sample, while 16 to 19 samples contain only lime. The unidentifiable grains are not taken into account.

The groups based on colour and the groups based on identifiable grains do not show much resemblance.

Sample	Colour	Consolidation chunks (mm)	Grains Identifiable					Unidentifiable
A.1	7.5Y 8/1 - lg	S	B		C?			
A.2	5Y 7/3 - ly	S	B	L S	C?	GR		
Ba.1	5Y 8/3 - py	L ≤1 cm	B	L	C?	GR		
Ba.2	5Y 8/3 - py	L ≤1 cm		L				Black, red-brown
Ba.3	5Y 8/3 - py	L ≤5 mm		L				Quartz, orange-brown, dark gray
Ba.4	10YR 8/1 - lg	L ≤5 mm		L				Small red-brown grains. Green-gray mat. ≤1 cm.
Bb.1	7.5Y 8/1 - lg	L ≤5 mm	B	L	C?	GR		
Bb.2	7.5Y 8/1 - lg	L ≤1.5 cm	B	L	C			
Bb.3	7.5Y 8/1 - lg	S	B		C			
Bc.1	7.5Y 8/1 - lg	L ≤2 cm	B	L	C?			Dark gray
Bc.2	7.5Y 8/1 - lg	L ≤1 cm		L	C?			Orange, gray brown
Bc.3	7.5Y 8/1 - lg	L ≤2 cm		L S			O	Black, red-brown, white
Bc.4	10Y 8/1 - lg	S	B	L S				Black
Bc.5	7.5Y 8/1 - lg	L ≤3 mm		L				Small black, gray, red-brown
D.1	2.5Y 7/4 - ly	L ≤1 cm		L				Black, brown, red
D.2	2.5Y 7/4 - ly	L ≤1 cm	B	L				Black, brown, red
Va.1	10YR 8/1 - lg	L ≤1 cm		L				Some black, dark brown, gray
Vb.1	5Y 8/2 - lg	L ≤7 mm		L		GR		
Vb.2	5Y 8/2 - lg	L ≤5 mm		L	C	GR		
Vc.1	7.5Y 8/1 - lg	L ≤1.5 cm						Black, orange-red
Vc.2	7.5Y 8/1 - lg	L ≤1 cm					O(wood)	Some white, red-brown, gray
Vc.3	5Y 8/2 - lg	L ≤2 cm						Black, dark brown-gray, orange, white
Vd.1	2.5Y 8/2 - lg	L ≤1 cm		L	C			
Vg.1	7.5Y 8/1 - lg	S+L		L		GR		
Vn.1	7.5Y 8/1 - lg	L ≤5 mm						Black, gray and red-orange-brown, white
Vo.1	5Y 8/2 - lg	L ≤1 cm		L	C?			Gray
Vs.1	2.5Y 8/2 - lg	L ≤1 cm						Some brown, gray
Vw.1	5Y 8/3 - py	L ≤5 mm		L				Black, orange, white. Black mat. ±3 mm.
W.1	7.5Y 8/2 - lg	L		L				Dark gray, dark red-brown
W.2	7.5Y 8/1 - lg	L		L				Dark gray, dark red-brown
W.3	7.5Y 8/1 - lg	L ≤5 mm		L				Dark gray, dark red-brown
W.4	5Y 8/2 - lg	S		L		GR		Dark gray, red, white
W.5	2.5Y 8/6 - y	L ≤1 cm		L				Brown, gray
W.6	7.5Y 8/1 - lg	L ≤1 cm						Some white, dark
Zc.1	7.5Y 8/2 - lg	L ≤2 cm		L	C?			Red, gray
Zc.2	7.5Y 8/1 - lg	L ≤1.5 cm		L				Quartz, dark gray, red-brown
Zc.3	7.5Y 8/1 - lg, 5Y 6/2 - go	S	B					Quartz
Zc.4	2.5Y 7/1 - lg	S	B					
Zc.5	7.5Y 8/2 - lg	L ≤2 cm		L				Dark gray, red
Zc.6	5Y 8/2 - lg	S		L				Black, red
Zc.7	10YR 7/2 - dyr	S	B	L				Quartz, black, brown
Zc.8	2.5Y 8/3 - py	L ≤1.5 cm	B	L		GR		Black, brown
Zc.9	5Y 7/3 - ly	L ≤1.5 cm		L				Some black, brown, red
Zc.10	7.5Y 8/2 - lg	S	B	L				Gray
Zw.1	7.5Y 8/2 - lg	S+L		L S			O	Dark gray-brown
Zw.2	5Y 8/2 - lg	S						Gray, red, white
Zw.3	7.5 8/1 - lg	S	B	L		GR		Black
Zw.4	5Y 8/2 - lg	S		L				

Table 5.1: Results of the macroscopic analysis.
Colour: g: gray(ish), o: olive, r: orange, y: yellow, d: dull, l: light, p: pale.
Consolidated: L: loose material, S: stone.
Grains: B: brick, L: lime, S: shell, C: (char)coal, GR: gray rock, O: organic.

Colour	Samples
2.5Y 7/1 (light gray)	Zc.4.
2.5Y 7/4 (light yellow)	D.1, D.2.
2.5Y 8/2 (light gray)	Vd.1, Vs.1.
2.5Y 8/3 (pale yellow)	Zc.8.
2.5Y 8/6 (yellow)	W.5.
5Y 6/2 (grayish olive)	Zc.3?
5Y 7/3 (light yellow)	A.2, Zc.9.
5Y 8/2 (light gray)	Vb.1, Vb.2, Vc.3, Vo.1, W.4, Zc.6, Zw.2, Zw.4.
5Y 8/3 (pale yellow)	Ba.1, Ba.2, Ba.3, Vw.1.
7.5Y 8/1 (light gray)	A.1, Bb.1, Bb.2, Bb.3, Bc.1, Bc.2, Bc.3, Bc.5, Vc.1, Vc.2, Vg.1, Vn.1, W.2, W.3, W.6, Zc.2, Zc.3?, Zw.3.
7.5Y 8/2 (light gray)	W.1, Zc.1, Zc.5, Zc.10, Zw.1.
10Y 8/1 (light gray)	Bc.4.
10YR 7/2 (dull yellow orange)	Zc.7.
10 YR 8/1 (light gray)	Ba.4, Va.1.

Table 5.2: Groups made based on sample colour.

Combination identifiable grains	Amount of samples	Samples
none	6	Vc.1, Vc.3, Vn.1, Vs.1, W.6, Zw.2
B	2/3	A.1?, Zc.3, Zc.4
L	16/17/18/19	Ba.2, Ba.3, Ba.4, Bc.2?, Bc.5, D.1, Va.1, Vo.1?, Vw.1, W.1, W.2, W.3, W.5, Zc.1?, Zc.2, Zc.5, Zc.6, Zc.9, Zw.4
O	1	Vc.2
B C	1/2	A.1?, Bb.3
B L	4/5	Bc.1?, Bc.4, D.2, Zc.7, Zc.10
L C	1/2/3/4	Bc.2?, Vd.1, Vo.1?, Zc.1?
L G	3	Vb.1, Vg.1, W.4
L O	2	Bc.3, Zw.1
B L C	1/2	Bb.2, Bc.1?
B L G	3/4/5	A.2?, Ba.1?, Bb.1?, Zc.8, Zw.3
L C G	1	Vb.2
B L C G	1/2/3	A.2?, Ba.1?, Bb.1?

Table 5.3: Groups made based on the presence of the five identifiable grains. B: brick, L: lime, C: (char)coal, G: gray rock, O: organic.

The samples of the groups with the colours 2.5Y 7/4 (D.1 and D.2), 2.5Y 8/2 (Vd.1 and Vs.1) and 5Y 7/3 (A.2 and Zc.9) are not in a group based on identifiable grains with the same samples of that group.

Two samples (Vb.1 and W.4) with the colour 5Y 8/2 contain only lime and gray rock, two (Vc.3 and Vw.2) contain none of the identifiable grains and two maybe three (Zc.6, Zw.4, Vo.1?) contain only lime.

Three (Ba.2, Ba.3 and Vw.1) out of four samples with the colour 5Y 8/3, two, maybe three, (W.1, Zc.5, Zc.1?) out of five samples with the colour 7.5Y 8/2 and the two samples (Ba.4 and Va.1) with the colour 10YR 8/1 contain only lime as identifiable grain. This is the largest group, so it is not strange that a large part of the samples from various groups based on colour are in this group.

The samples with the colour 7.5Y 8/1 form 5 groups based on identifiable grains. A.1 forms a group with either Zc.3 or Bb.3 (depending on whether coal is present). Furthermore, two samples contain brick, lime and gray rocks (Bb.1 and Zw.3), two samples contain brick, lime and coal (Bb.2 and Bc.1), four or five samples contain only lime (Bc.5, W.2, W.3, Zc.2, Bc.2?), and three none of the identifiable grains (Vc.1, Vn.1 and W.6).

Concluding, the two sets of groups do not match. The groups based on identifiable grains are more significant than the groups based on colour, since colour is more subjective than grain content.

5.2 Microscopic analyses

Thin sections were made of 16 samples: A.1, A.2, Bc.4, Vg.1, Vc.3, W.4, Zc.1, Zc.3, Zc.4, Zc.6, Zc.7, Zc.10, Zw.1, Zw.2, Zw.3, Zw.4. Unfortunately, the other samples had only loose material, so no thin sections could be made of them.

The articles of Elsen (2006), Pavia et al. (2008), the theses of Kootker (2007a and b) and the book of Wenk and Bulahk (2004) are used for interpretation of the features that have been observed. Illustrations of Pettijohn et al. (1987) and Terry and Chilingar (1955) were used to estimate respectively sorting and sphericity, and percentage.

All photo's in this section have been taken by the author, using a microscope with 39x magnification.

5.2.1 Descriptions

A.1

Matrix: Light brown in PPL, dark brown in XPL, slightly lighter with than without compensator.
Minerals and Aggregates:

- Quartz. The minerals are mostly angular, 0.03-0.2 mm, well sorted. In addition, a polycrystalline quartz mineral has been seen. About 35 % of the total.
- Shells. One shell is probably of a snail (Gastropoda) (fig. 5.1 left) The material is carbonate: brown in PPL and XPL (with and without compensator). The holes are not filled, except for 2 round black objects. The diameter is about 0.3 mm.
  An other object that is probably a piece of a shell is brown in PPL and colourful in XPL (the same with and without compensator). The size is about 0.7 mm.
- Probably charcoal. A few pieces that are black in PPL and XPL (with or without compensator.) Some are more dense than others. Some are round, but most are angular, 0.05-0.5 mm. The minerals can also be other organic material or iron oxides.
- Lime lumps. These objects are slightly darker or lighter than the matrix and contain less aggregates. Until about 1mm.

- Calcite. The mineral shows various cracks, it seems to be broken. It is gray in PPL, it is light yellow with green en pink spots and it has a black extinction in XPL. In XPL with the compensator, it is yellow/green with a pink extinction. The shape is round, has a diameter of about 0.3 mm. It has a white, black or pink rim. This piece of calcite is not well burned compared to the matrix. Similar smaller minerals (about 0.05 mm) are present throughout the sample.
- Unknown, about 0.2 mm. Green or yellow in PPL, slightly more gray in XPL, orange/green in XPL with compensator.
- Unknown, about 0.2 mm. Yellow in PPL, black in XPL, pink/red in XPL with the compensator. Angular.
- Unknown, about 0.2 mm. White in PPL, light yellow in XPL (with or without compensator).
- Unknown, about 0.1 mm. Brown/white in PPL, blue in XPL, green to purple in XPL with compensator.
- Unknown. A mineral that is brown in PPL and XPL, about 0.3 mm, cleavage in one direction, no pleochroism and extinction. It has orange and green lines in XPL with the compensator. It resembles biotite, although biotite has pleochroism.

Pores: Some small pores of about 0.1 mm, some round pores of about 0.5 mm, some irregular pores of about 1mm and one long crack of 4x0.5 mm. In total about 5% of the volume.
Binder/Aggregate (B/A) ratio: 60/40

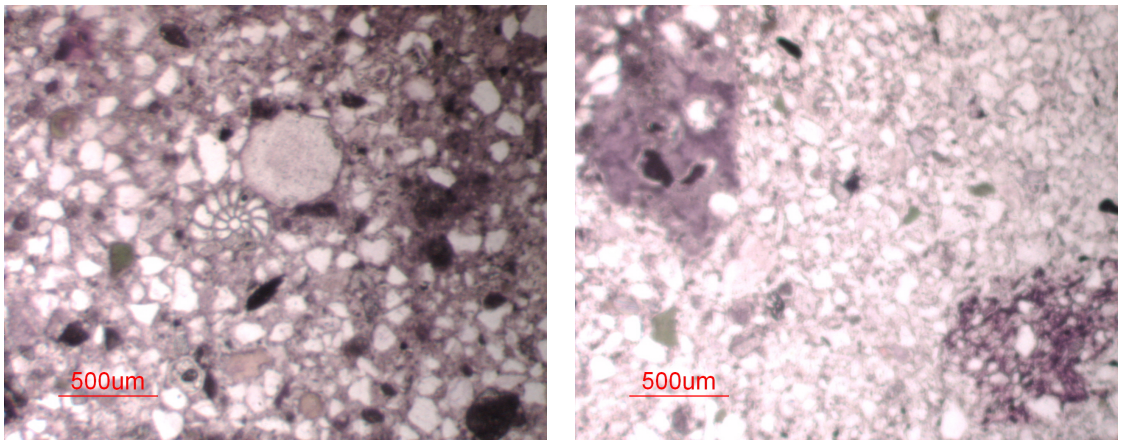

Figure 5.1: Left: Shell at A.1, PPL. Right: Lime lump (left) and brick (right) at A.2, PPL.

A.2

Matrix: Not much is present. Light brown in PPL, brown/grayish in XPL.
Minerals and Aggregates:

- Quartz. Angular, 0.03-0.1 mm, well sorted. About 55%.
- Charcoal. A few angular fragments occur from 0.1-0.3 mm in diameter.
- Ceramic fragments (fig. 5.1 right). Pieces that are red/brown in PPL, and slightly darker in XPL. At least four large fragments and a few smaller ones are present, the largest being 0.9x0.6 mm, a smaller one for example 0.5x0.3 mm. Quartz is present in them. They can be recognized as ceramics with the naked eye, because of their orange colour.
- Lime lumps (fig. 5.1 right). At least two large brown lumps are present, 1.3x0.8 mm and 2.3x0.6 mm. They are darker than the matrix, slightly darker in XPL than in PPL and slightly lighter with compensator than without compensator. Quartz and dark brown pieces are present in them.

- A mineral is present which seems to be calcite. It is a rounded mineral, 0.8x0.6mm, gray in PPL, partly brown and partly very colourful with partly a black extinction (purple with compensator) in XPL.
  The lime lumps and calcite are white when looking to the thin section with the naked eye.
- Unknown. About 0.05 mm. Brown in PPL, dark brown in XPL, dark purple in XPL with compensator.
- Unknown. About 0.05 mm. Light brown in PPL, yellow/orange with black extinction in XPL and yellow with purple extinction in XPL with compensator.
- Unknown. Light green in PPL, more gray in XPL, very colourfull in XPL with compensator. About 0.1 mm. This might be the same mineral as the green mineral in A.1.

Pores: Some pores between 0.5 and 2 mm are present. These have rounded to irregular shapes and are spherical to elongated. In addition, some pores of about 0.1 mm are present. In total about 3%.
B/A ratio: 40/60

Bc.4

Matrix: Dark brown in PPL and XPL.
Minerals and Aggregates:

- Many angular quartz grains. Larger than at the previous two samples: 0.1-0.2 mm, medium sorting. About 40% of the total.
- Many shell fragments (fig. 5.2 left). The one in the photo seems to be from the Ensis genus, a Bivalvia class. 0.5x0.2 to 2.0x0.8 mm. These are brown in PPL. Some are brown and some are pink and green in XPL. They have an black extinction without and a purple with compensator in XPL.
- Carbonate lumps. These slightly lighter brown than the matrix in PPL, slightly darker in XPL without and lighter with compensator. Darker spots and pores are present in most lumps. E.g. 0.6x0.3 or 1.7x1.0 mm.
- Some unburned calcite is present, small minerals that are white or yellow in PPL and show bright colours in XPL. About 0.1-0.4 mm.
- Unknown. About 0.3mm. Brown in PPL, yellow-green in XPL without compensator, green-orange in with compensator. They might be the same as the unknown green minerals in A.1.

Pores: Many pores of various sizes, from only 0.1 mm to almost 3x0.5 mm. All have irregular borders. Some are more spherical, while some are more elongated. About 30% of the total.
B/A ratio: 50/50

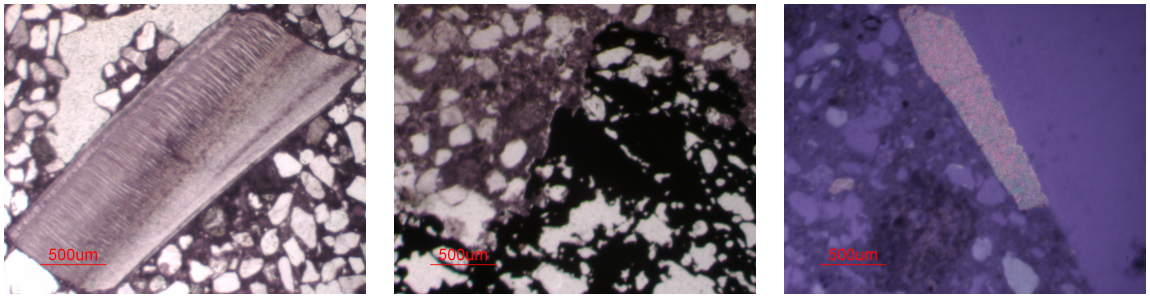

Figure 5.2: Left: Shell at Bc.4, PPL. Middle: Charcoal fragment at Vc.3, PPL. Right: Calcite (top) and lime lump (bottom) at Vc.3, XPL.

Vc.3

Matrix: The matrix is brown in PPL, slightly darker in XPL.
Minerals and Aggregates:

- Quartz. Angular grains, 0.05-0.3 mm, medium sorting. Some small polycrystalline quartz is present. About 30% of the total.
- Charcoal (fig. 5.2 middle). A large black area of 4.4x3.8 mm, is visible which contains many pores. In addition, charcoal is visible as small dense black pieces.
- Shell. A thin (0.1 mm) fragment is present of 1.5 mm long.
- Carbonate lumps are present. Some show pores or small black spots. Some show cracks. One shows a black rim. E.g. 0.6x0.5 mm.
- Calcite mineral (fig. 5.2 right). Elongated mineral of 1.4x0.3 mm. White with brown spots at PPL. It exists of small yellow, orange, pink, green and blue spots in XPL, every 90 degrees there is a black extinction without compensator and a pink extinction with compensator. This calcite mineral was not burned. In addition, some calcite minerals of about 0.2 mm are present.

Pores: Many small pores (about 0.3 mm) and a few larger ones (about 1 mm) are present. About 10% of the volume.
B/A ratio: 65/35

Vg.1

Matrix: Dark brown in PPL and XPL. Similar to that of Bc.4.
Minerals and Aggregates:

- Many angular quartz grains, 0.1-0.3 mm, medium sorting. Some small polycrystalline quartz. Except for some carbonate lumps and small other minerals, quartz is the only mineral present, it is estimated to be about 48% of the total.
- Carbonate lumps are visible throughout the sample. They are slightly lighter than the mortar. Some show pores or darker spots. E.g. 0.6x0.4 mm.
- Probably ceramics: a dark brown, almost black material. It is overlapped by a carbonate lump (fig. 5.3 left). The total of the two minerals is 1.1x0.9 mm.
- Unknown. A mineral that looks like quartz, except it is yellow/orange in XPL without a compensator instead of white. About 0.3 mm.

Pores: Many large pores. Some connected cracks seem to be in the same direction. These cracks are about 0.5 mm thin, and in total about 6 mm long. Their borders are irregular. Also some smaller pores are visible (0.2-0.5 mm). About 30% of the volume.
B/A ratio: 50/50

W.4

Matrix: Light brown in PPL, darker in XPL.
Minerals and Aggregates:

- An area with more and darker matrix and larger quartz grains can be seen (fig. 5.3 right). This might be a piece of old re-used mortar. 11x8 mm.
- Quartz. Most are angular, but some are round. 0.05-0.3 mm, poorly sorted. About 40%. The quartz grains are slightly larger in one area than at the other.
- Charcoal. Dense black pieces of about 0.3 mm.

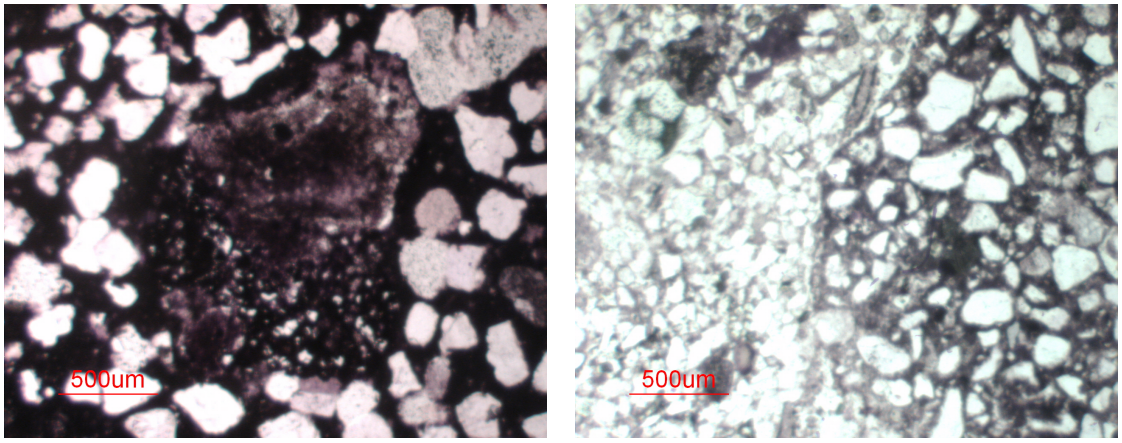

Figure 5.3: Left: Carbonate lump (top) and ceramics (bottom) at Vg.1, PPL. Right: Two areas with different mortar at W.4, PPL.

- Lime lumps. Brown minerals, which are slightly darker in XPL. Some minerals are slightly lighter than average, some slightly darker. Some have pores and cracks. The lumps are white with the naked eye. Until 2 mm.
- Probably calcite. Some very small (0.05 mm) minerals which are white in PPL and have very high-order interference colours in XPL are visible.
- Unknown material. Grey brown in PPL, orange to gray with partially black extinction in XPL. With the compensator blue, yellow and red lines are visible. The object exists of small coloured lines with various directions. Black spots (charcoal) are visible in the material. 1.8x0.6 mm. It resembles calcite, except calcite shows high-order interference colours in XPL, while this mineral shows only orange and gray.

Pores: A large triangle shaped pore with an irregular border of 4x2 mm. Some medium pores of 0.5-1 mm and many small pores of about 0.1-0.2 mm, spherical to elongated, with irregular to sharp borders. In total about 10% of the volume.
B/A ratio: 50/50

Zc.1

Matrix: Light brown material in PPL, gray in XPL, brown in XPL with compensator.
Minerals and Aggregates:

- Quartz. All kind of shapes, angular and round. 0.05-0.3 mm, poorly sorted. About 50% of the total.
- A shell. Probably from a snail (Gastropoda). 1.3x0.9 mm. (fig. 5.4 left). The shell is filled with mortar, e.g. quartz, charcoal and matrix.
- Charcoal. One large fragment of 1 mm. In addition, some dark minerals which might be charcoal as well as lime fragments.
- Lime lumps. One is a triangle, but most are more rounded. Some are very large (e.g. 1.8x1.4 mm). They are about the same colour as the matrix. They are white with the naked eye.
- Calcite. Some small (0.05-0.1 mm) minerals which are white in PPL and have very high-order interference colours in XPL.
- Unknown. Some of the green minerals that has already been seen in sample A.1. About 0.2 mm.

- Unknown. A mineral that is yellow in PPL, black in XPL and pink/red in XPL with the compensator. It resembles the second unknown mineral of A.1, but also the unknown green mineral. About 0.2 mm.
- Some areas with few matrix and many small quartz minerals (<0.03 mm) are present.

Pores: Some pores of small (0.1 mm) to medium size (0.5-1 mm) are present. Most have an irregular border. From spherical to elongated. About 5% of the total.
B/A ratio: 45/55

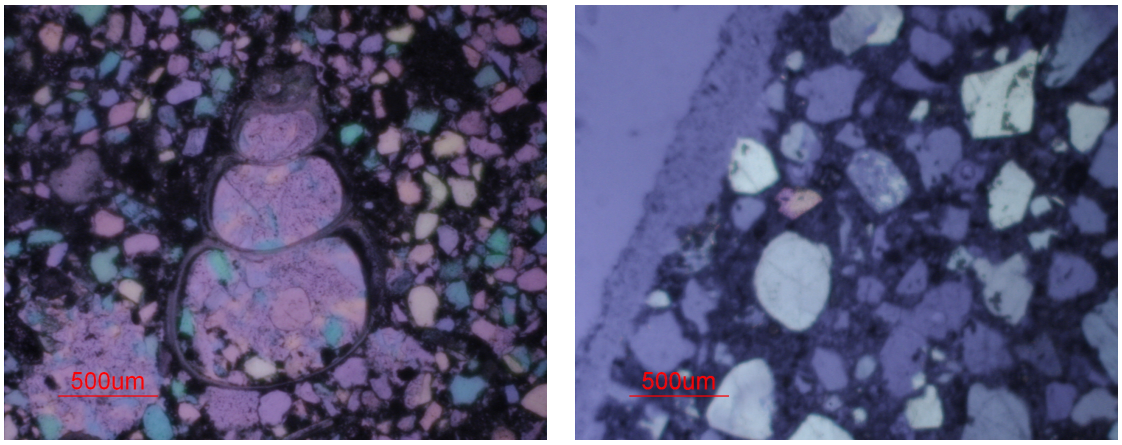

Figure 5.4: Left: Shell at Zc.1, XPL with compensator. Right: Quartz at Zc.3, XPL.

Zc.3

Matrix: Dark brown material.
Minerals and Aggregates:

- Quartz (fig. 5.4 right). Very round to very angular, 0.05x0.05 to 1.8x1.2 mm, very poorly sorted. Some are light brown instead of white, but they seem to be quartz when looking to them in XPL with the compensator. Much polycrystalline quartz is present. About 48% of the total.
- Unknown. Some minerals that are white in PPL, red/orange with a black extinction in XPL (fig. 5.4(b), orange to pink to brown to dark green in XPL with compensator. About 0.2-0.5 mm. One is orange/pink in XPL, green/yellow/orange/pink with compensator and has a diameter of 0.2 mm.
- Unknown. Some minerals that are light brown in PPL, dark brown in XPL without and purple in XPL with compensator. This might be very thin material, since pores are black in XPL without and purple with compensator, maybe a lime fragment. About 0.5 mm.

Pores: Some pores of about 0.1 to 0.5 mm are visible, from very round to very angular. About 5% of the total.
B/A ratio: 50/50

Zc.4

Matrix: Brown.
Minerals and Aggregates:

- Quartz. Angular, small: 0.05-0.1 mm, well sorted. About 20% of the total.
- Lime lumps (fig. 5.5 left). They have the same colour as the matrix. Some show cracks and pores. Some are very large, e.g. 3.6x5.4 mm, but most are about 0.5 mm in diameter.

- A shell has been observed. About 0.3x0.2 mm.
- Calcite. Some small (0.1 mm) fragments.
- Unknown. Some green minerals, similar to those in A.1. About 0.1 mm.
- Unknown. Some minerals that are yellow/orange/red in PPL, slightly darker in XPL without and red/orange/pink in XPL with compensator. About 0.1 mm.

Pores: Many pores which are smaller than 0.1 mm and some pores between 0.3 and 1 mm. Most have sharp borders, they range from well rounded to very angular. In addition, thin cracks can be seen in the mortar and lime lumps. About 10% of the volume.
B/A ratio: 60/40

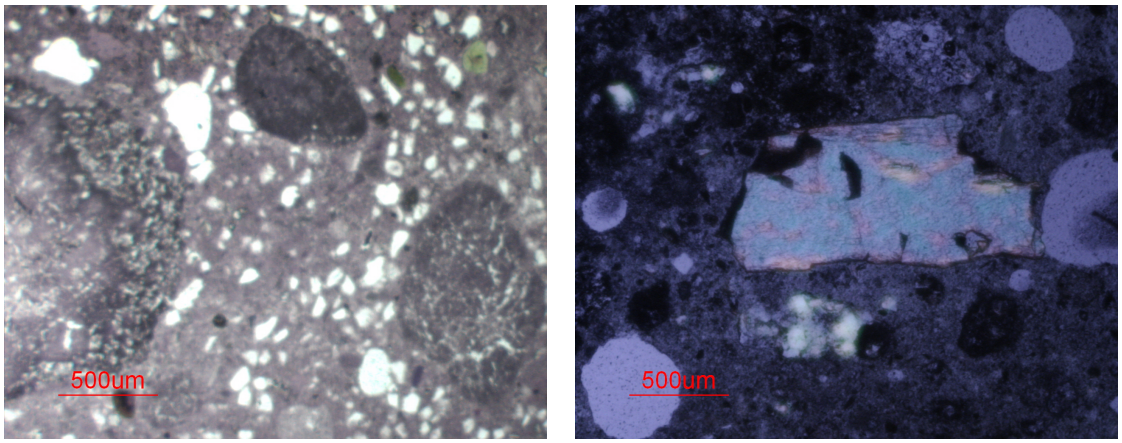

Figure 5.5: Left: Lime lumps at Zc.4, PPL. Right: Pyroxene at Zc.6, XPL.

Zc.6

Matrix: Brown.
Minerals and Aggregates:

- Quartz. Less minerals than in most other samples, about 10%. Most are very angular, 0.05-0.4 mm, poorly sorted. In addition to normal quartz minerals, polycrystalline quartz is present with a size ranging from 0.03 to 0.1 mm.
- Charcoal. Some pieces that are black in PPL and XPL. 0.1-1 mm.
- Pyroxene (fig. 5.5 right). Two similar minerals are present. One is white in PPL, while the other is light yellow. One has stripes in one direction, while the other shows clear double cleavage. They are bright blue with brown extinction in XPL, they contains orange, yellow and purple spots. Blue with pink, orange, yellow spots in XPL with the compensator, and a light green to orange to pink extinction. The largest contains a few dark brown spots and is 1.2x0.6 mm.
  An other pyroxene is brown in PPL, the same colour as the matrix. It has a blue to yellow birefringence in XPL. It is orange/yellow to blue/green in XPL with the compensator. It is L shaped and has a hole in it. This mineral is 0.5x0.6 mm.
- Unknown. Some small pieces that are brown/orange/red/yellow in PPL and XPL. One has a diameter of 0.5 mm and has an arc shape. Others are 0.1-0.3 mm.
- Unknown. A mineral that is gray in PPL and yellow in XPL. About 0.1 mm.
- Some spots appear to be less dense. It are not pores, but the matrix is much lighter. Various sizes until 6 mm.

Pores: Pores of 0.1 to 1.5 mm. Most are very round, some have a more angular shape. Some long thin cracks are present. In total about 10%.
B/A ratio: 80/20

Zc.7

Matrix: Brown.
Minerals and Aggregates:

- Quartz. Larger and more round than in most thin sections. 0.05-1.0 mm, poorly sorted. Much polycrystalline quartz (fig. 5.6 left). Some grains are light brown in PPL, but act the same as quartz in XPL, as at Zc.3. About 68%.
- Unknown. Some small minerals that are white/gray in PPL and red or orange in XPL. About 0.05 mm. The same unknown minerals as in Zc.3.
- Unknown. Minerals which are light brown in PPL, black in XPL without compensator and purple with. The same minerals as in Zc.3. Possibly a not dense lime fragment. About 0.5 mm.

Pores: The amount of pores is larger than the amount of matrix. The aggregates lay largely in pores instead of matrix. About 60% of the total.
B/A ratio: 30/70

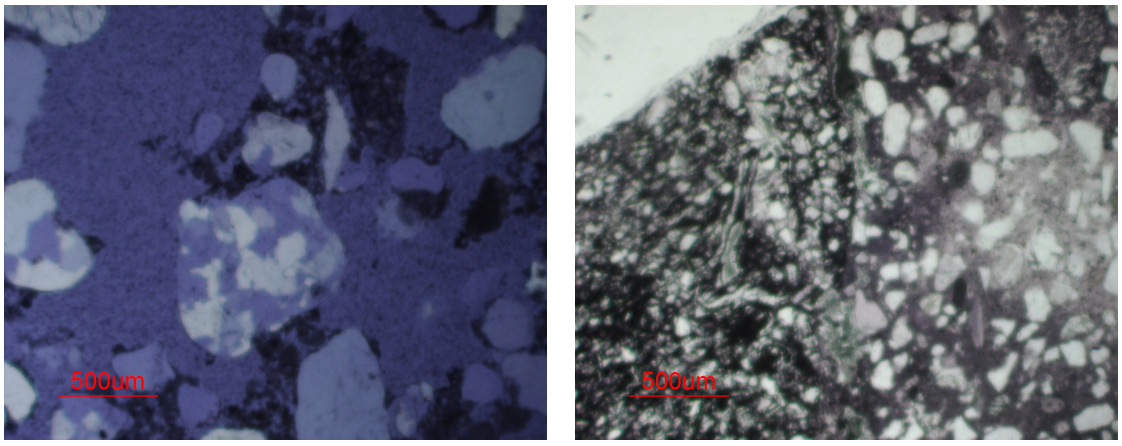

Figure 5.6: Left: Polycrystalline quartz at Zc.7, XPL. Right: Brick (left) at Zc.10, PPL.

Zc.10

Matrix: Brown, variating between slightly lighter and darker brown.
Minerals and Aggregates:

- Quartz. Some rounder, some more angular, 0.03-0.3 mm, poorly sorted. About 35%.
- Lime lumps. From 0.3x0.3 to 2.5x0.9 mm. The same colour as the matrix. Some show cracks and pores.
- An area that is black in PPL and XPL. It contains much quartz. When looking to the thin section with the naked eye, it is orange/red and it seems to be a piece of brick (fig. 5.6 right). 2.8x1.8 mm.
- Calcite. Some small (0.1-0.2 mm) minerals that show high-order interference colour in XPL.
- Unknown. Some minerals that are green in PPL and slightly darker green in XPL. In XPL with the compensator, they are dark green with a yellowish extinction. About 0.1mm in diameter. This is the same unknown green material as in A.1.

Pores: Some small (about 0.1 mm) and some larger (0.5-1 mm) pores are present. Some are very large: 4-5 mm long. About 20% of the total.
B/A ratio: 55/45

Zw.1

Matrix: Dark brown.
Minerals and Aggregates:

- Quartz. From very rounded to very angular, 0.03-0.5 mm, poorly sorted. About 45%.
- Lime lumps (fig. 5.7 left). Some are slightly lighter or darker than the matrix. Many show cracks. Most are between 0.5 and 1 mm.
- A mineral that is black in PPL, XPL and with the naked eye. Probably charcoal. About 0.7 mm.
- Calcite. Some minerals that are white and gray in PPL and very colourful in XPL. E.g. 0.7x0.5 or 0.5x0.2 mm. Also some smaller (about 0.1 mm) minerals are present.
- Unknown. Some small minerals which are green/yellow in PPL, dark green in XPL and brown/green/orange in XPL with compensator. The same minerals as in A.1. 0.1-0.3 mm.

Pores: Some small pores of about 0.1 mm, some are slightly larger: 0.5 mm. The largest pores are in lime lumps. Most have irregular borders. About 5%.
B/A ratio: 50/50

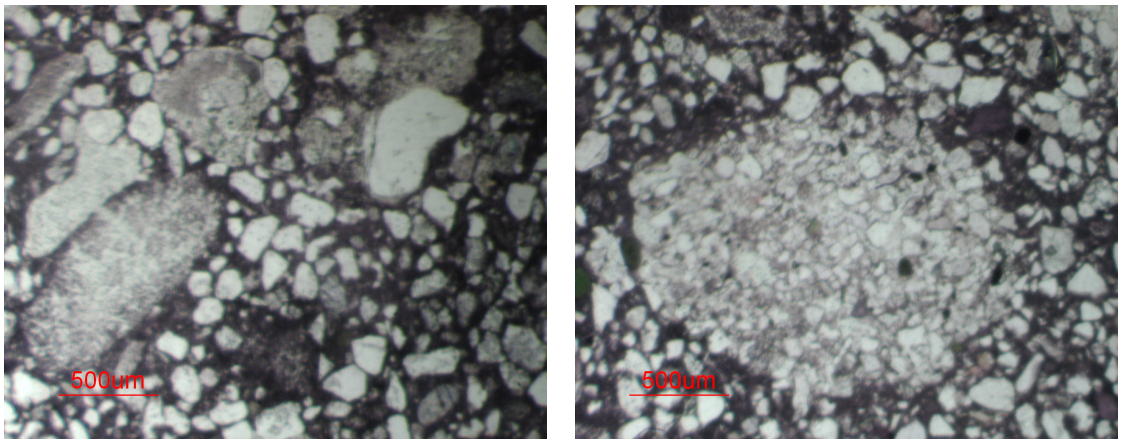

Figure 5.7: Left: Lime lumps at Zw.1, PPL. Right: Area with quartz at Zw.2, PPL.

Zw.2

Matrix: Brown.
Minerals and Aggregates:

- Quartz. Mostly angular, some are round. 0.03-0.3 mm, poorly sorted. About 40%.
- Areas with a lighter matrix, smaller quartz fragments and many pores (fig. 5.7 right). This might be old re-used pieces of mortar. One of 3.6x2.0 mm and one of 1.5x1.0 mm.
- Lime lumps. Some are broken and are very porous. Some are slightly lighter or darker than the matrix. 0.1-1.5 mm.
- Calcite. Minerals that are white and gray in PPL and very colourful in XPL. About 1.0x0.7 mm. Some calcite minerals might be slightly burned, since they are less colourful and more brown than the other minerals.
- Unknown. Minerals which are green in PPL and darker green in XPL, as in sample A.1.

Pores: Some small pores (0.1-0.3 mm), some are larger (around 0.5 mm), one pore is 4.5 mm long. Most have irregular borders. Many pores are in lime lumps. In total about 20% of the volume.
B/A ratio: 50/50

Zw.3

Matrix: Brown.
Minerals and Aggregates:

- Quartz. Angular and round, 0.05-0.3 mm, poorly sorted. Some polycrystalline quartz is present. About 50%.
- Lime lumps (fig. 5.8 left). Large brown minerals. They contain many cracks and pores. From very small until about 2 mm.
- Calcite (fig. 5.8(a). Minerals that are brown in PPL and colourful in XPL. E.g. 0.6x0.3 or 0.8x0.4 mm.
- Unknown. Some minerals that are light green in PPL and darker green in XPL. 0.1-0.2 mm. The same unknown green minerals as in A.1.
- Unknown. Black material, round and angular minerals, about 0.05-0.5 mm. Possibly charcoal or very dark carbonate lumps.

Pores: Some small pores (around 0.1 mm), some larger ones (0.5-1.0 mm). Most have irregular borders. Some are in lime lumps. In total around 10%.
B/A ratio: 40/60

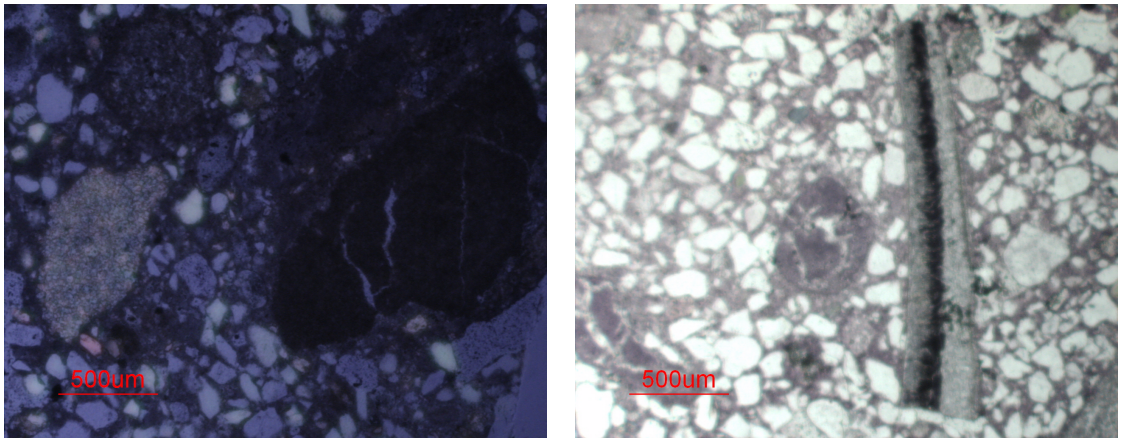

Figure 5.8: Left: Calcite (left) and carbonate lump (right) at Zw.3, XPL. Right: Shell and lime lumps at Zw.4, PPL.

Zw.4

Matrix: Brown.
Minerals and Aggregates:

- Quartz. Angular and round. Poorly sorted, 0.03 to 1.0 mm in diameter, with an average of 0.1 mm. About 50%.
- Two pieces that seem to be shell (fig. 5.8 right). They are brown in PPL and brown with small yellow, pink, orange and green spots in XPL. 1.5x0.3 and 1.4x0.1 mm.
- Lime lumps (fig. 5.8 right). Slightly lighter or darker than the matrix. They show many cracks. Until 2.5 mm.
- Calcite. Minerals that are white/brown in PPL and colourful in XPL. From 0.2 to 2.5 mm.
- Charcoal. At least one angular mineral of 0.5 mm. Some other black to dark brown minerals might be charcoal or dark carbonate fragments. Some minerals are very round.

- Unknown. Some minerals are present, which are light green in PPL and slightly darker in XPL. About 0.1 mm. These are the same minerals as in sample A.1.

Pores: Many pores ranging from 0.1 to 4 mm, most are between 0.1 and 1 mm. Most have irregular borders, some are in lime lumps. In total about 10% of the volume.
B/A ratio: 40/60

5.2.2 Discussion and conclusion

The binder is carbonate in all samples. This carbonate with grains less than 4 microns is called micrite, or lime mud (Nichols, 2009). The colour differs between lighter and darker brown in PPL and XPL.

Quartz grains are present in all samples, in different sizes and shapes. Polycrystalline quartz, which consists of aggregates of crystals instead of single crystals (Pettijohn et al., 1987), is present in seven samples (A.1, Vc.3, Vg.1, Zc.3, Zc.6, Zc.7 and Zw.3).

Lime lumps are present in thirteen samples (all except Zc.3, Zc.6 and Zc.7), calcite in twelve (all but Vg.1, Zc.3, Zc.6 and Zc.7) charcoal in eight or nine (A.1, A.2, Vc.3, W.4, Zc.1, Zc.6, Zw.1, Zw.3?, Zw.4)), shells in six (A.1, Bc.4, Vc.3, Zc.1, Zc.4 and Zw.4), ceramic fragments in three (A.2, Vg.1 and Zc.10), areas with a different kind of mortar in two samples (W.4 and Zw.2) and pyroxene in only one sample (Zc.6) (see table 5.4).

Most unknown minerals are very small and not important for grouping. Some are observed in more than one sample.

The green mineral that is lighter in PPL, slightly darker in XPL without compensator and orange/green with compensator is present in the samples A.1, A.2, Bc.4, Zc.1, Zc.4, Zc.10, Zw.1, Zw.2, Zw.3 and Zw.4.

Two unknown minerals are present in Zc.3 and Zc.7. Minerals which are white/gray in PPL and red/orange in XPL and minerals which are light brown in PPL, dark brown/black in XPL without compensator and purple with compensator. The last might be a thin lime fragment.

	Ratios		Quartz				Other Aggregates							
Sample	Pores (%)	B/A (%)	Amount (%)*	Shape	Size (mm)	Sorting	P.Q.	Lime	Calcite	Charcoal	Shell	Ceramics	Old mortar?	Pyroxene
A.1	5	60/40	35	a	0.03-0.2	well	+	+	+	+	+			
A.2	3	40/60	55	a	0.03-0.1	well		+	+	+		+		
Bc.4	30	50/50	40	a	0.1-0.2	med.		+	+		+			
Vc.3	10	65/35	30	a	0.05-0.3	med.	+	+	+	+	+			
Vg.1	30	50/50	48	a	0.1-0.3	med.	+	+				+		
W.4	10	50/50	40	a-r	0.05-0.3	poor		+	x	+			+	
Zc.1	5	45/55	50	a-r	0.05-0.3	poor		+	x	+	+			
Zc.3	5	50/50	48	va-vr	0.05-1.8	poor	+							
Zc.4	10	60/40	20	a	0.05-0.1	well		+	x		+			
Zc.6	10	80/20	10	va	0.05-0.4	poor	+			+				+
Zc.7	60	30/70	68	r	0.05-1.0	poor	+							
Zc.10	20	55/45	35	r-a	0.03-0.3	poor		+	x			+		
Zw.1	5	50/50	45	va-vr	0.03-0.5	poor		+	+	+				
Zw.2	20	50/50	40	a-r	0.03-0.3	poor		+	+				+	
Zw.3	10	40/60	50	a-r	0.05-0.3	poor	+	+	+	?				
Zw.4	10	40/60	50	a-r	0.03-1.0	poor		+	+	+	+			

Table 5.4: Overview of the ratios, aggregates and minerals in samples detected by microscopy. *Percentages quartz of the total minus the pores. Abbreviations: a:angular, r:round, v:very, med.: medium, P.Q: Polycrystalline quartz. x: only a small amount of calcite is present.

In order to group the samples, the matrix, presence of aggregates and quartz characteristics are compared with each other.

Zc.3 and Zc.7 are similar. Both contain almost only quartz, further they contain polycrystalline quartz and two unknown minerals. The grains are larger and rounder than in other samples. Since Zc.7 is modern mortar, Zc.3 should be modern mortar as well. In retrospect, it looks as modern mortar when looking at it macroscopically.

Zc.1, Zc.10 and the Zw samples are similar since they have a dark matrix and the B/A ratio is about the same. The binder of Zw.4 is slightly lighter than that of the others. The quartz is of about the same size, poorly sorted and can be angular or rounded. Lime and calcite are present in every sample.

The area of W.4 that is different from the rest of the sample seems also to be similar to this group, especially to Zw.1. They have the same matrix colour and the same size quartz minerals. They contain lime, calcite and charcoal. Only Zw.1 contains the unknown green mineral, while W.4 does not. The rest of W.4 seems to be more similar to A.1 in matrix colour and grains size. A.1 contains polycrystalline quartz and 2 small pieces of shell, while W.4 does not and W.4 contains a piece of old mortar, while A.1 does not. Furthermore, they differ in location, period and building owner, so it is not likely that this is the same mortar.

Zc.1 and Zw.4 are similar since they both contain lime, calcite, charcoal, shell and the unknown green mineral.

Furthermore, some samples contain the same aggregates, but their appearance is not the same.

A.1 and Vc.3 contain the same aggregates: polycrystalline quartz, lime, calcite, charcoal and shell. The appearance of the two samples is not the same, since Vc.3 contains slightly more binder than A.1, the quartz grains are slightly larger and the lime lumps are much larger. A.1 contains the unknown green mineral, while Vc.3 does not.

Bc.4 and Zc.4 contain lime, calcite, shell and the unknown green mineral. The appearance of the two samples is not the same, since the matrix of Zc.4 is lighter than that of Bc.4, the B/A ratio is larger and the quartz grains of Bc.4 are much smaller.

Summarizing, Zc.3 and Zc.7 make a group and W.4, Zc.1, Zc.10 and the Zw samples make a group. W.4 and Zw.1 form subgroup 1 and Zc.1 and Zw.4 form subgroup 2 of the last group, since they contain the same minerals.

5.3 TGA

The results of the TGA analyses are shown in table 5.5. This table presents the amount of salts, structurally bound water (SBW), CO_2, carbonates and the hydraulicity index (CO_2/SBW). According to Moropoulou et al. (2000), non-hydraulic mortar has a CO_2/SBW ratio above >10. All samples have a ratio <10, so all samples are hydraulic or near hydraulic.

The relation between the hydraulicity (CO_2/SBW) and the amount of CO_2 is presented in figure 5.9 left. Various groups can be seen in the graph, the lines which make these groups can be drawn from the lower left to the upper right corner of the graph (fig. 5.9 right).

The first line that can be seen is a long line from the lower left to the upper right corner of the graph. This group contains the samples A.2, D.1, Vb.1, Vo.1, W.5, Zw.3 and Zw.4. The second group is a small and dense group at the upper right, containing the samples Va.1, Zc.4, Zc.5, Zc.10 and Zw.2. The third group is a broad group, laying in the middle. Although it looks like a rest group, the samples show a direction. It contains the samples A.1, Ba.1, Bb.1,

Sample	Weight loss (wt.%) at temperature range (∘C)				CO_2/SBW
Measures loss of:	120-200 salts	200-600 SBW	600-1000 CO_2	615-1000 carbonates	
A.1	0.95	4.85	15.53	35.45	3.20
A.2	0.26	2.55	4.68	10.70	1.84
Ba.1	2.92	8.47	21.21	49.85	2.51
Ba.2	0.98	9.99	26.01	60.93	2.60
Ba.3	1.36	8.07	26.62	62.92	3.30
Ba.4	0.54	8.57	30.91	71.45	3.60
Bb.1	0.88	6.84	23.15	52.30	3.38
Bb.2	0.72	5.97	27.97	63.55	4.69
Bc.1	1.05	7.65	34.39	78.31	4.50
Bc.2	1.22	7.28	35.45	80.71	4.87
Bc.3	1.98	11.09	17.08	39.03	1.54
Bc.4	1.18	11.45	20.49	46.83	1.79
Bc.5	1.23	8.26	26.90	61.74	3.26
D.1	1.55	13.03	3.94	10.83	0.30
D.2	0.93	12.26	12.13	29.24	0.99
Va.1	1.12	4.70	28.43	64.14	6.04
Vb.1	0.44	2.96	22.17	50.47	7.49
Vb.2	0.76	7.95	12.33	27.74	1.55
Vc.1	1.14	11.38	16.79	41.33	1.47
Vc.2	0.62	7.65	24.28	55.88	3.17
Vc.3	2.76	8.78	12.53	30.84	1.42
Vd.1	0.81	13.22	14.13	32.40	1.07
Vg.1	1.43	12.95	27.46	63.19	2.12
Vn.1	1.49	15.92	16.26	38.29	1.02
Vo.1	0.46	3.16	15.03	34.13	4.76
Vs.1	1.01	7.85	28.21	64.96	3.60
Vw.1	1.77	9.25	26.71	61.95	2.89
W.1	0.53	8.74	21.54	48.76	2.46
W.2	0.47	6.10	27.86	63.41	4.57
W.3	0.61	5.48	20.43	46.31	3.73
W.4	0.55	4.06	16.73	38.00	4.12
W.5	0.66	2.95	19.02	43.22	6.45
W.6	0.99	7.39	14.99	34.05	2.03
Zc.1	1.19	8.94	14.10	32.34	1.58
Zc.2	1.98	5.59	24.23	55.86	4.33
Zc.3	2.61	7.33	10.71	24.45	1.46
Zc.4	0.52	4.50	30.27	68.95	6.73
Zc.5	0.24	4.44	28.72	65.09	6.47
Zc.6	3.02	6.47	14.73	33.48	2.28
Zc.7	0.96	6.56	21.21	47.82	3.23
Zc.8	3.17	9.48	9.82	22.26	1.04
Zc.9	0.55	6.96	16.74	38.05	2.40
Zc.10	0.74	4.46	29.36	66.81	6.58
Zw.1	1.11	5.70	25.05	56.76	4.39
Zw.2	0.44	4.76	27.97	63.64	5.88
Zw.3	0.43	2.85	28.12	63.89	9.87
Zw.4	0.41	2.97	29.36	66.25	9.89

Table 5.5: TGA results

Bb.2, Bc.3, Bc.4, D.2, Vb.2, Vc.1, Vc.2, Vc.3, Vd.1, Vn.1, W.1, W.2, W.3, W.4, W.6, Zc.1, Zc.2, Zc.3, Zc.6, Zc.7, Zc.8, Zc.9 and Zw.1. The fourth group is a small dense group, similar to group 2. The samples Ba.2, Ba.3, Bc.5 and Vs.1 and Vw.1 are present in this group. The last group contains 4 samples, Ba.4, Bc.1, Bc.2 and Vg.1, and is at the right of the graph.

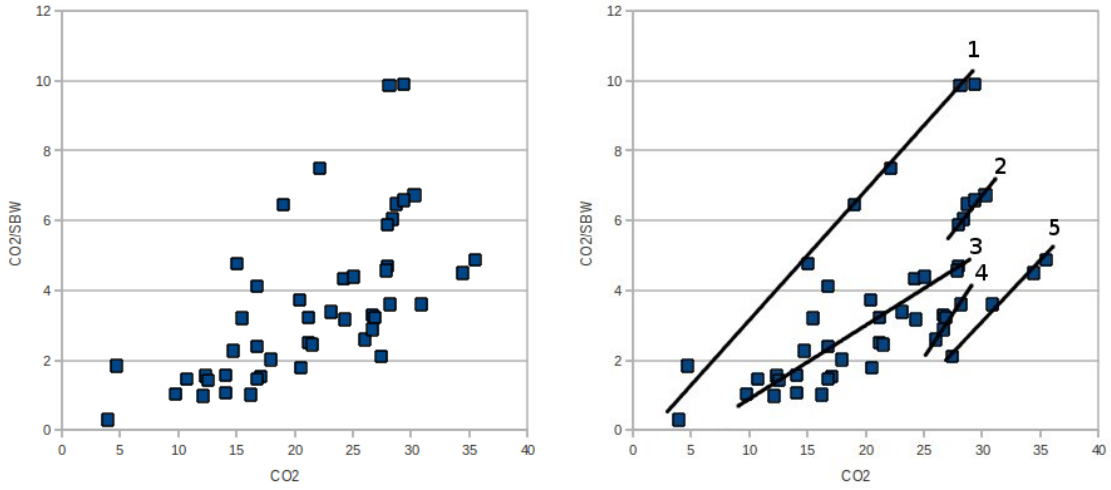

Figure 5.9: TGA results. Left: The hydraulicity of the samples. Right: Groups based on hydraulicity.

5.4 FT-IR

5.4.1 Basic knowledge

Before the data is analysed, it is studied which bands can be present in lime mortar and which bonds they represent. This paragraph shows an overview of these bands.

A band around 3430 cm^{-1} is present in all mortar samples, this is interpreted as a water peak (Genestar et al., 2006; Kootker, 2007b). One or more peaks can be visible.

The peaks at the wavelengths 1416-1430, 872-874 and 712-714 cm^{-1} are interpreted as calcite (Kootker, 2007b; Regev et al., 2010), a peak at 2514 cm^{-1} as carbonate (Bakolas et al., 1995; Silva et al., 2005; Gleize et al., 2009) and a peak at 1798-1800 cm^{-1} as a calciumcarbonate band (e.g. Silva et al., 2005; Gleize et al., 2009).

C-H bands, which are present in almost all organic compounds can be found in the region 3100-2700 cm^{-1} (Whittaker, 2000). Silva et al. (2005) interprets the peaks at 2920 and 2860 (fig. 5.10 left) which were found in mortar as organic material.

Peaks representing CO_2 are sometimes present around 2350 cm^{-1} (Socrates, 2001) since the instrument also measures some air. The blank should correct for this, but that may not have happened entirely.

Silicates, Si-O-Si bonds and quartz all belong to this Si-O group. Bands at the following wavelengths have been interpreted as bonds from the Si-O group: 1166 (Biscontin et al., 2002; Genestar and Pons, 2005), 1100-1000 (Socrates, 2001), 798 (Genestar and Pons, 2005; Kootker, 2007), 778 (Genestar and Pons, 2005) and 694 cm^{-1} (Biscontin et al., 2002; Genestar and Pons, 2005).

Band at the wavelength 470 and 536 cm^{-1} are interpreted as iron oxide (Genestar and Pons, 2005; Genestar et al., 2006; Kootker, 2007b). The band around 470 cm^{-1} is also interpreted as silicates (Kootker, 2007b) and an Al-O bond of clay (Kristof et al., 1993).

Bands at around 1685 (Rampazzi and Bugini, 2006), 1623-1621 (Genestar and Pons, 2005; Gomes et al., 2005; Rampazzi and Bugini, 2006), 1116 (Genestar, 2005; Kootker, 2007b), 660

(Gomes et al., 2005), 602 (Genestar and Pons, 2005; Kootker, 2007b) and 589 cm^{-1} (Genestar and Pons, 2005) have been interpreted as sulphate.

A band around 1638 cm^{-1} has been interpreted as brucite (Biscontin et al., 2002). This is a Mg hydroxides layer which occurs in some clays (Faure, 1998).

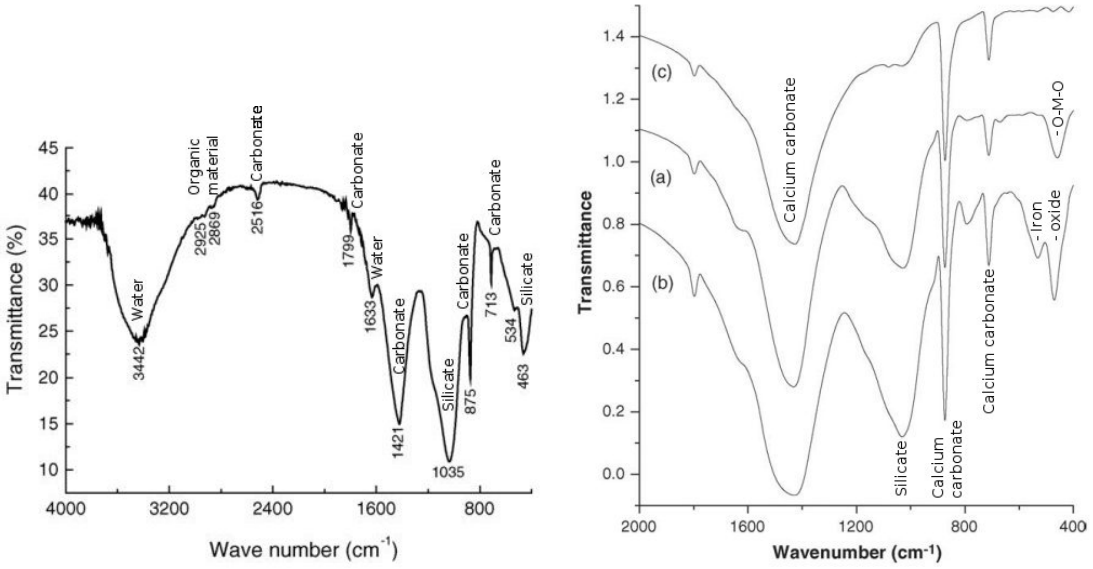

Figure 5.10: Left: An example of a FT-IR spectrum based on Silva et al., 2005. Right: Three types of mortar distinguished by relative size of the two largest peaks (Genestar et al., 2006).

5.4.2 Discussion and conclusion

The FT-IR spectra are very similar to each other. All spectra have a large **water** peak around 3430 cm^{-1}. Mostly one peak is visible, like at Zc.6 (fig. 5.12), but sometimes two or more peaks are visible, like at A.2 (fig. 5.11).

Calcite is present in all samples. All samples show peaks at the wavelengths 1416-1430, 872-874 and 712-714 and 2514 cm^{-1}. All spectra, except that of D.1, also show a peak at 1798-1800 cm^{-1}, which represents a calciumcarbonate band.

A peak at 2982-2986 cm^{-1} is present at most samples, as well as a peak at 2876-2878 cm^{-1}. These peaks probably represent **organic material**. Although not at 2920 and 2860 cm^{-1} the peaks seem quite similar to the peaks of organic material at the article of Silva et al. (2005). Sample A.2 does not show peaks near 2984 and 2876, but at 2934 and 2864 cm^{-1}, that is even closer to the peaks in the article (Silva et al., 2005). Bc.3 also lacks a peak near 2984, but shows peaks at 2964 and 2926 cm^{-1}. The spectrum of D.1 is the only one that does not show peaks between 3100-2700 cm^{-1}.

The peaks at around 2350 cm^{-1} are $\mathbf{CO_2}$ peaks caused by the instrument.

One or more bands which represent **Si-O** bonds are found in each sample, except for Zc.6. These bands than be observed near the wavelengths 1166, 1100-1000, 798, 778 and 694 cm^{-1}. The spectrum of Zc.6 does contain a peak at 994, that may belong to the 1000-1100 cm^{-1} range.

Iron oxide is present in W.6, Zc.9 and Zc.10 since the spectra of these samples show bands at 536 and around 470 cm^{-1} (Genestar and Pons, 2005; Genestar et al., 2006; Kootker, 2007b). A band around 470 cm^{-1}, which is indicative for either iron oxides, silicates or an Al-O bond of clay is present in more samples.

Sulphate is present in the samples Ba.1, Ba.2, Ba.3, Ba.4, Bb.2, Bc.1, Bc.2, Bc.3, Bc.4, Bc.5, Vb.2, Vg.1, Va.1, Vc.1, Vc.2, Vc.3, Vd.1, Vo.1, Vn.1, Vs.1, Vw.1, W.2, W.4, W.6, Zc.1, Zc.2, Zc.3, Zc.5, Zc.7, Zc.8, Zw.1. This is indicated by the present of one or more bands at bands around 1685, 1623-1621, 1116, 660, 602 and 589 cm^{-1}.

Brucite is present in D.1, D.2, Vg.1, Vn.1, Zc.6 and Zc.9, indicated by a band around 1638 cm^{-1}.

Table 5.6 presents an overview of the components. No connection can be seen between the presence or absence of the various components.

Four groups can be made when looking at the relative size of the two largest peaks of the spectra, the calcite peak around 1420 cm^{-1} and the silicate peak around 1030 cm^{-1} (or in the range from 994 to 1116 cm^{-1}). This is the most distinctive difference between the spectra. This characteristic has also been used for making groups in previous research (Genestar et al., 2006 (fig. 5.10 right).

Group 1

Group 1 consist only of the sample A.2 (fig. 5.11). This sample has a much smaller calcite peak at 1430, than a Si-O peak at 1032 cm^{-1}.

Group 2

The two peaks are of equal size at the samples of this group (fig. 5.12). The samples are: A.1, D.1, Zc.3, Zc.6 and Zc.8.

Sample D.1 is special, because it is the only one that does not show a $CaCO_3$ band at 1798-1800 cm^{-1}. It also does not show a peak which represents organic material between 3100-2700 cm^{-1}.

Sample Zc.6 does not contain silicate oxides, except for maybe the 994 cm^{-1} peak.

Group 3

The samples of this group have a Si-O band that is smaller than the calcite peak (fig. 5.13). Subgroups can be made of samples in which the Si-O peak is close to the calcite peak, like Vb.2, Vc.3 and Vo.1 and of samples with a small peak Ba.2, Zc.7, Zc.9, Zc.10, Zw.1, Zw.2, Zw.4. The following samples are between these subgroups: Ba.1, Ba.3, Bb.1, Bb.2, Bc.3, Bc.4, Bc.5, D.2, Va.1, Vb.1, Vc.1, Vc.2, Vd.1, Vn.1, Vs.1, W.1, W.3, W.4, W.5, W.6, Zc.1, Zc.2.

The three samples which contain iron oxide are in this group.

Group 4

At the samples of group 4 (fig. 5.14), the Si-O peak near 1030 cm^{-1} is very small and sometimes almost completely gone. The samples in this group are Ba.4, Bc.1, Bc.2, Vg.1, Vw.1, W.2, Zc.4, Zc.5, Zw.3.

Sample	Water	Calcite	Silicium oxides	Organic mat.	Iron oxide	Sulphate	Brucite	
A.1	+	+	+	+				
A.2	+	+	+	+				
Ba.1	+	+	+	+		+		
Ba.2	+	+	+	+		+		
Ba.3	+	+	+	+		+		
Ba.4	+	+	+	+		+		
Bb.1	+	+	+	+				
Bb.2	+	+	+	+		+		
Bc.1	+	+	+	+		+		
Bc.2	+	+	+	+		+		
Bc.3	+	+	+	+		+		
Bc.4	+	+	+	+		+		
Bc.5	+	+	+	+		+		
D.1	+	+	+				+	
D.2	+	+	+	+			+	
Va.1	+	+	+	+		+		
Vb.1	+	+	+	+				
Vb.2	+	+	+	+		+		
Vc.1	+	+	+	+		+		
Vc.2	+	+	+	+		+		
Vc.3	+	+	+	+		+		
Vd.1	+	+	+	+		+		
Vg.1	+	+	+	+		+	+	
Vn.1	+	+	+	+		+	+	
Vo.1	+	+	+	+		+		
Vs.1	+	+	+	+		+		
Vw.1	+	+	+	+		+		
W.1	+	+	+	+				
W.2	+	+	+	+		+		
W.3	+	+	+	+				
W.4	+	+	+	+		+		
W.5	+	+	+	+				
W.6	+	+	+	+	+	+		
Zc.1	+	+	+	+		+		
Zc.2	+	+	+	+		+		
Zc.3	+	+	+	+		+		
Zc.4	+	+	+	+				
Zc.5	+	+	+	+		+		
Zc.6	+	+		+			+	
Zc.7	+	+	+	+		+		
Zc.8	+	+	+	+		+		
Zc.9	+	+	+	+	+		+	
Zc.10	+	+	+	+	+			
Zw.1	+	+	+	+		+		
Zw.2	+	+	+	+				
Zw.3	+	+	+	+				
Zw.4	+	+	+	+				

Table 5.6: FT-IR results

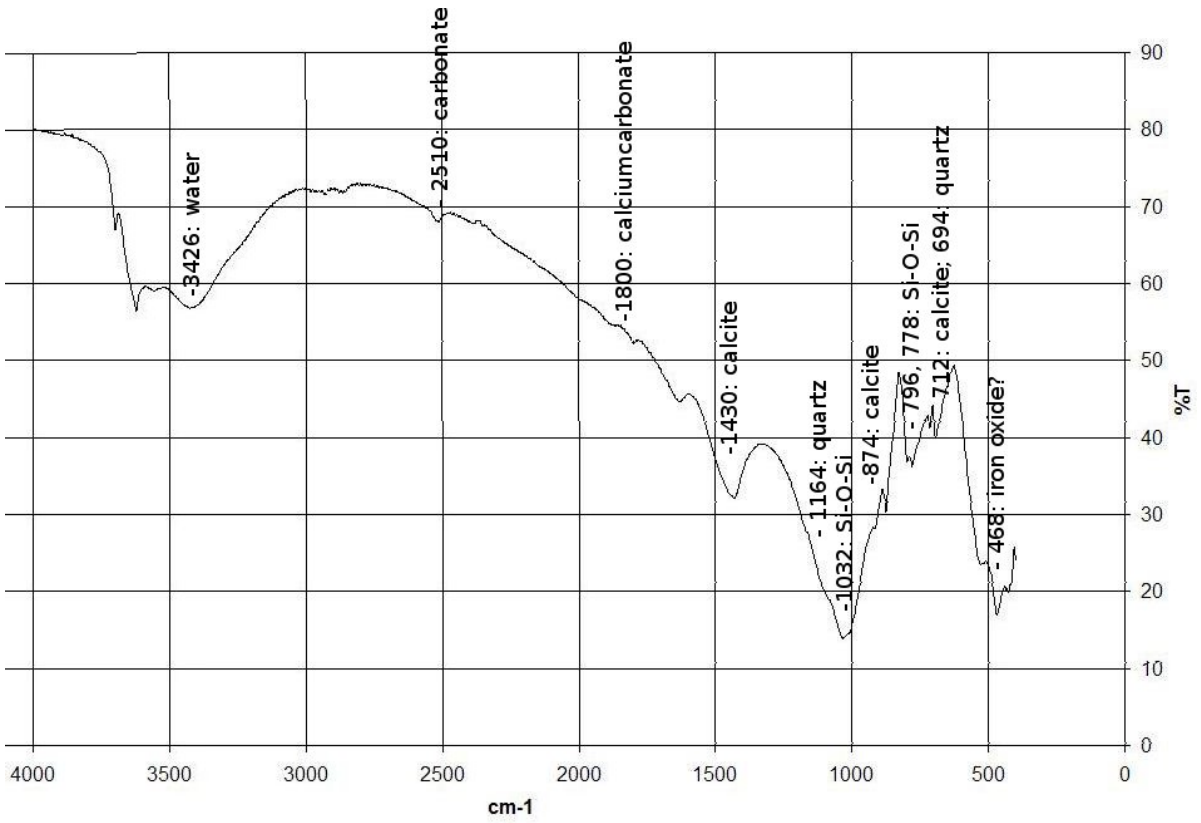

Figure 5.11: FT-IR group 1 (A.2).

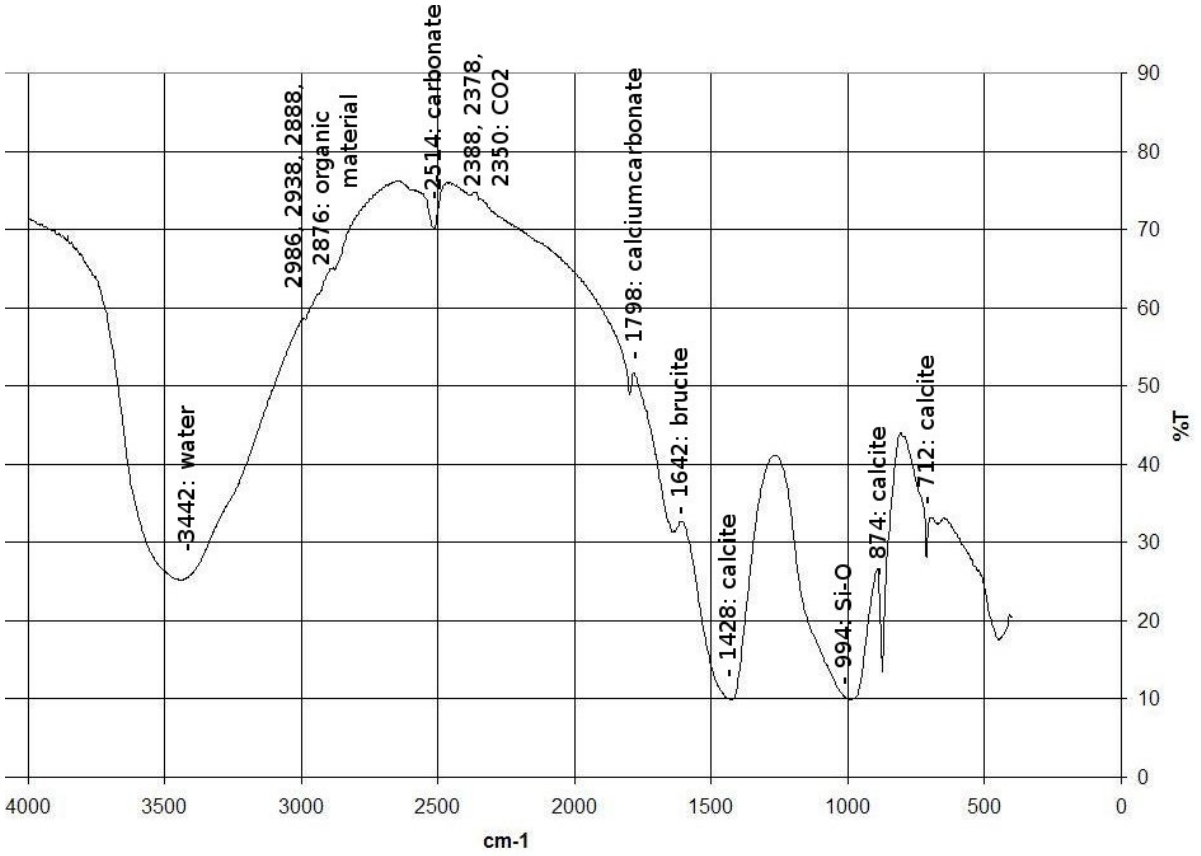

Figure 5.12: FT-IR group 2 (Zc.6).

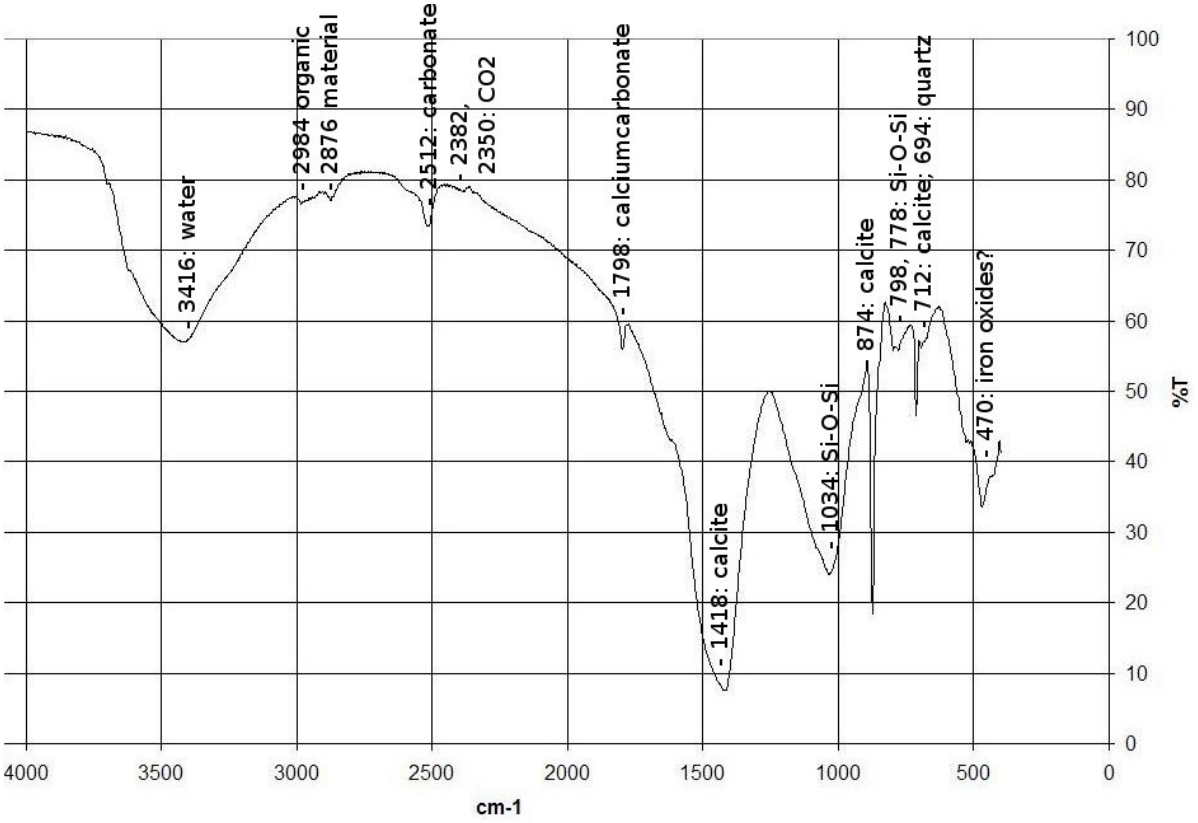

Figure 5.13: FT-IR group 3 (W.4).

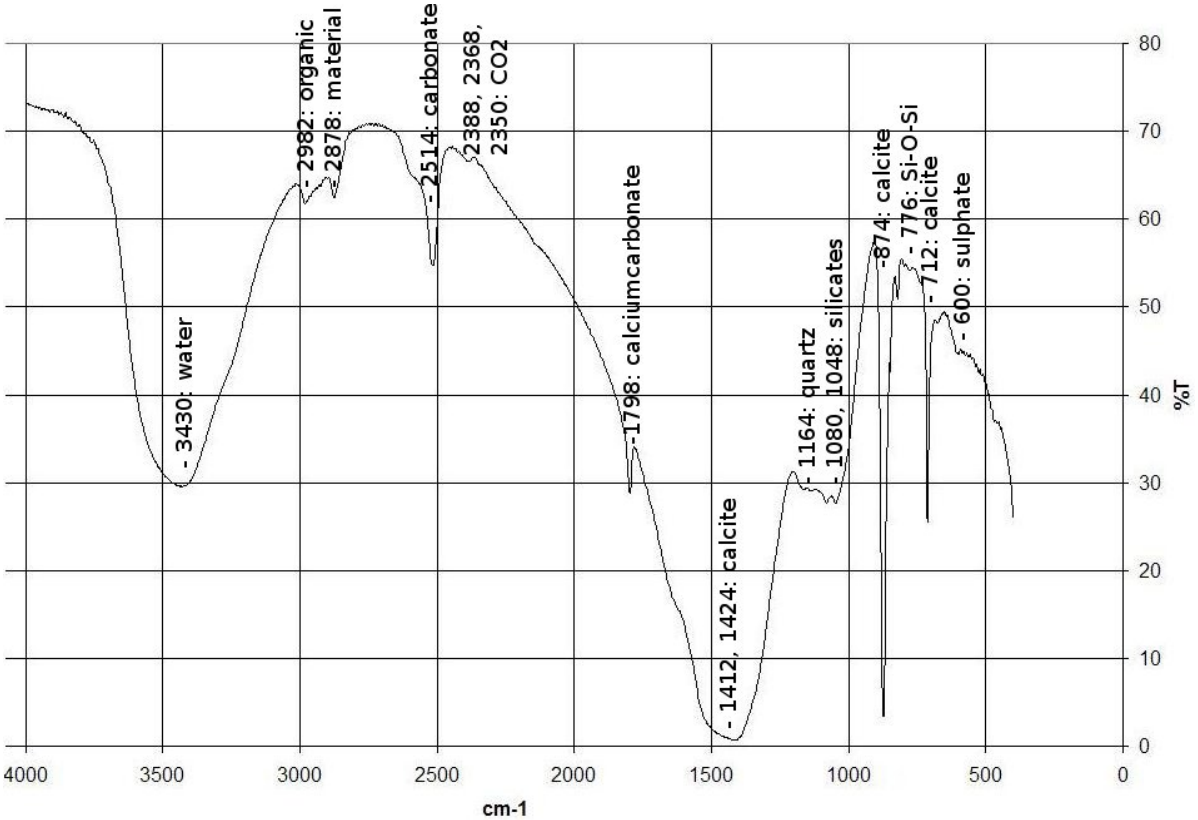

Figure 5.14: FT-IR group 4 (Bc.1).

Chapter 6

Discussion

6.1 Macroscopy

Fourteen groups could be made based on colour (table 5.2) and thirteen groups based on the presence of five identifiable grains (table 5.3).

A link between the macroscopic results based on the sample colour and the site and building can be seen at the samples of 'Ter Doest' which are both in the same group. All three samples from the abbot's house and four out of five samples from the 18^{th} century barn at 'Ten Bogaerde' have the same colour. In addition, three out of four samples from the medieval barn of 'Ten Bogaerde' have the same colour. The samples from the other sites and buildings are too scattered throughout the groups.

The samples from the Cistercian and non-Cistercian buildings are mixed. All groups containing more than three samples contain samples from buildings being built by the Cistercians and samples of buildings which are not built by the Cistercians.

A link between the date of the building and the colour of the material can not be seen clearly. All four samples with the colour 5Y 8/3 are from the 13^{th} century, but three of these samples are from the same location ('Ten Bogaerde'), so it is not clear whether the relation between these samples is based on location or date. Five samples with the colour 7.5Y 8/1 are from the 17^{th} century, but these are also all from 'Ten Bogaerde'.

Following, the groups based on grain content are compared with the site and building of the sample. The only match is that four out of six samples which contain no identifiable grains are from Veurne. Furthermore, the group which only contains lime contains four or five samples out of twelve samples from 'Ten Bogaerde', four out of six samples from Wulveringem and six out of fourteen samples from 'Hof de Zande'. It is logical that this group contains a large part of these samples, since it is the largest group.

It is noticeable that all samples which contain no identifiable grains are not from Cistercian buildings. The samples which contain brick alone, brick and lime, lime and organic material or brick, lime and coal are all from Cistercian buildings.

A link between grain content and date can not be seen. The most obvious fact is that seven or eight out of sixteen or nineteen samples are from the 13^{th} century, but these samples are from only three sites, so the location may have influence on this.

6.2 Microscopy

Quartz source

Sediment transported by rivers is the most angular, beach sand is more round and sediment transported by aeolian processes is the roundest (Chorley et al., 1985). The sediment transported by a river becomes more round downstream. Quartz is very durable compared to other minerals (McBride and Dane Picard, 1987).

Suspension, at which the grain does not touch the surface, is not effective in rounding particles, while traction, at which the grain does touch the ground, is (Twenhofel, 1945). Traction occurs at larger and denser grains than suspension and when there is lower velocity in the water (Nichols, 2009). Experimental stream transport studies have shown that quartz gravel becomes round after 161 km, while quartz sand becomes round after a greater distance (Chorley et al., 1985). Grains smaller than 0.5 mm, which is the case here, need to travel thousands of miles when they are transported by aqueous traction before they are rounded (Twenhofel, 1945).

The quartz grains in most samples are angular or angular to round, so this quartz has been transported by rivers. The longest river in the area is the Scheldt. This river is about 350 km, including the Western Scheldt, which is about 160 km long (International Scheldt Commission, 2011). The quartz grains are still angular when they have been transported along this distance. Aendijcke and Kloosterzande are nearby the Scheldt. The largest river near 'Ten Bogaerde', Veurne and Wulveringem is the river Yser. This river is 78 km long (Provoost, 1997), so the quartz grains in this river are still angular.

The modern sample Zc.7 is the only sample that contains round quartz grains. Since these grains are very large compared to grains in other samples, it is more likely they have a marine than an aeolian provenance.

Comparison with site, building, date and building owner

Two groups are found based on the microscopic analyses. The samples of the first group, Zc.3 and Zc.7, are from the same Cistercian site and building and are both modern. All samples of group 2 are from 'Hof te Zande', except W.4. The samples of subgroup 2a, W.4 and Zw.1, have no common site, building, date (12^{th} and 17^{th} century) and building owner. The samples of subgroup 2b, Zc.1 and Zw.4, have a common Cistercian site and date (13^{th} century), but are from different buildings. The other samples of group 2 (Zc.10, Zw.2 and Zw.3) are from the same Cistercian site and date and from two buildings.

The other samples, also those which have a common location, date and building owner, were not similar to each other. For example, Zc.4 and Zc.6 have the same location and date as Zc.1 and Zw.4, but are different.

6.3 TGA

Comparison with literature

Using TGA, a distinction can be made between hydraulic and non-hydraulic mortar. This distinction is based on the amount of SBW (structurally bound water), which is indicative for hydraulic compounds, and CO_2, which is indicative for carbonates. Non-hydraulic mortar, or typical lime mortar, shows a SBW value <3% (Moropoulou et al., 2003), a CO_2 value between 33 and 40% and a CO_2/SBW ratio above >10 (Moropoulou et al., 2000), while hydraulic mortar shows a SBW value >3.5%, a CO_2 value <30% and a CO_2/SBW value <6 (Moropoulou et al., 2000).

The results in Table 5.5 show that none of the samples has a CO_2/SBW value higher than 10. Only the samples Zw.3 and Zw.4 are very close with values of 9.87 and 9.89. The samples

that have a SBW value <3% are: A.2, Vb.1, W.5, Zw.3 and Zw.4. The samples that have a CO_2 value between 33 and 40% are: Bc.1 and Bc.2. Therefore, none of the samples is typical lime mortar, only Zw.3 and Zw.4 are nearby.

The samples that have a SBW value >3.5% are all samples, except for the samples mentioned before and Vo.1, which has a value of 3.16. The samples that have a CO_2 value <30% are all samples except for Bc.1, Bc.2 (mentioned before) and Ba.4 and Zc.4. The samples that have a CO_2/SBW value <6 are all samples except for Vb.1, Va.1, W.5, Zc.4, Zc.5, Zc.10, Zw.3 and Zw.4.

Concluding, the samples that are hydraulic according to Moropoulou et al. (2000) are A.1, Ba.1, Ba.2, Ba.3, Bb.1, Bb.2, Bc.3, Bc.4, Bc.5, D.1, D.2, Vb.2, Vg.1, Vc.1, Vc.2, Vc.3, Vd.1, Vn.1, Vs.1, Vw.1, W.1, W.2, W.3, W.4, W.6, Zc.1, Zc.2, Zc.3, Zc.6, Zc.7, Zc.8, Zc.9, Zw.1, Zw.2, while the other samples are between the hydraulic and non-hydraulic group.

The two groups are plotted in figure 6.1, together with the samples of Moropoulou et al. (2003), from which the classification came. The group of hydraulic mortars seems to be one group, but the group of the samples between non-hydraulic and hydraulic seems to be more the outliers of the first group than a second group. They are not near the group of typical lime mortars measured by Moropoulou et al. (2003), except for the samples Zw.3 and Zw.4.

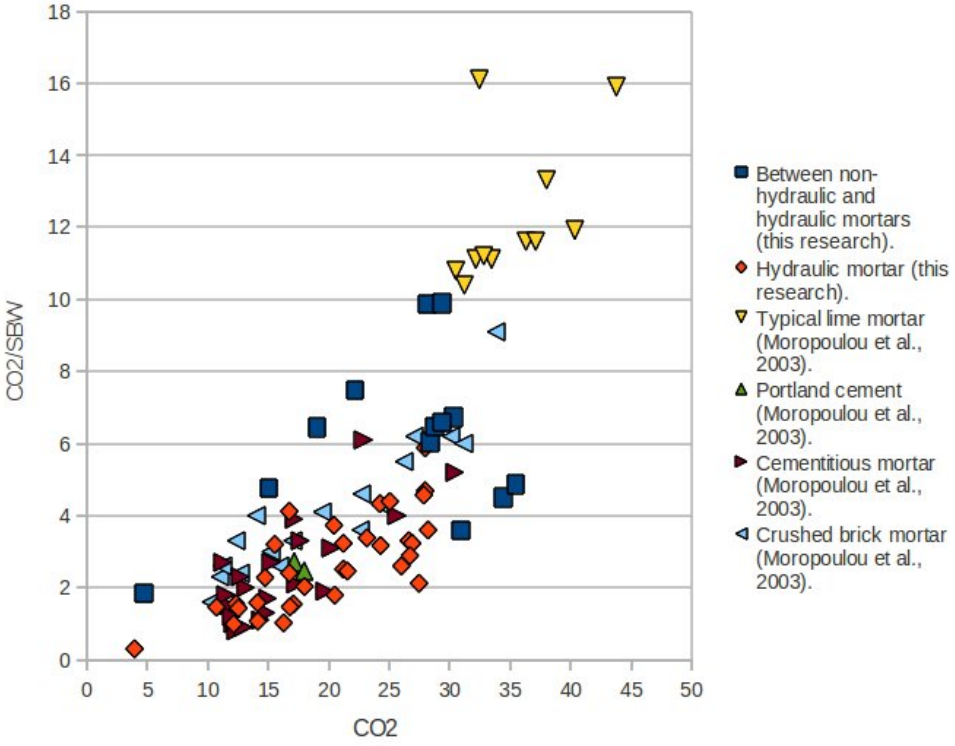

Figure 6.1: TGA results compared with Moropoulou et al. (2003).

The classification of the samples by Moropoulou et al. (2003) was done on samples from the Mediterranean, instead of on samples from Belgium and The Netherlands. This may be the reason that some samples do not fit between the boundaries of the hydraulic mortar and the typical lime mortar.

That most mortars are hydraulic means that relative few carbonate is present compared to hydraulic compounds. For example pieces of brick, which have been seen under the microscope at a few samples, help to increase the hydraulicity.

Comparing TGA results with site, building, date and building owner

The TGA results can be grouped by site (fig. 6.2 upper left). Group A, D and Z show clear diagonal lines, while group B, V and W are much broader. It is logical that the group made from the samples from Veurne is very large, since this group contains many different buildings.

When the results are grouped by building (fig. 6.2 upper right), the church (Zc) and wall (Zw) of 'Hof te Zande' and the medieval (Ba) and 18^{th} century (Bc) barns of 'Ten Bogaerde' show clear diagonal lines. The other groups contain either too few samples or are broader.

No clear relation can be observed between the TGA results and the date of the buildings (fig. 6.2 lower left). The samples of the 13^{th} and 17^{th} century seem to show a diagonal line like at the location graph, but this may be influenced by the locations, since most of the samples of 'Hof te Zande' are from the 13^{th} and 17^{th} century. The samples of the 18^{th} century barn of 'Ten Bogaerde' show differences in hydraulicity per building phase. The samples from the older building phase (Bc.3, Bc.4, Bc.5) are hydraulic mortars according to Moropoulou et al. (2003), while the samples from the newer phase (Bc.1 and Bc.2) are not. The average estimated date is taken for this graph.

The TGA results from the Cistercian buildings overlap with the results of the other buildings (fig. 6.2 lower right). The results from the Cistercian buildings show a thiner line than that of the other buildings, but that could be caused by the locations. The samples of 'Hof te Zande' are more grouped, than the samples from Veurne and Wulveringem. Concluding, no relation can be seen between the initiators of the building and the TGA results form the mortar.

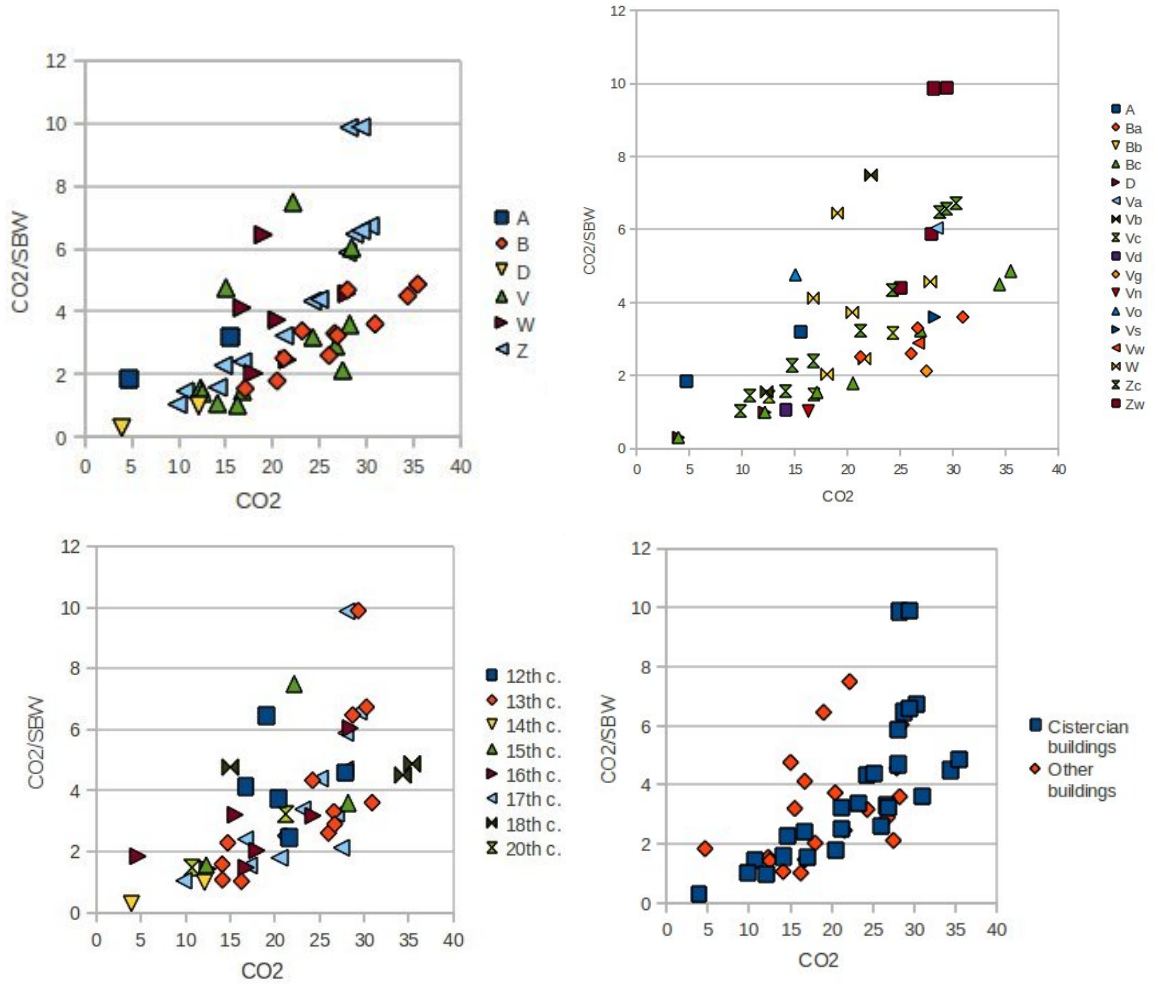

Figure 6.2: TGA results grouped by site (upper left), building (upper right), date (lower left) and building owner (lower right).

The amount of salt in the samples may also be linked to the location of the site. All Wulveringem (W), Aendijcke (A) and Bb samples have between 0 and 1 weight % salts, while the Bc samples contain between 1 and 2 % salts.

6.4 FT-IR

The measured bonds are often indicative for more than one component.

Clay occurs in many forms. Its basic formula is the formula of kaolinite, which is $Al_2Si_2O_5(OH)_4$ (Faure, 1998). This consist out of the bonds O-H, Si-O-Si, Si-O-Al, Al-O-H (Genestar and Pons, 2005) and Si-O (Kristof et al., 1993). Brucite is a group of Mg hydroxides, which can be present in clay instead of Al hydroxides (Faure, 1998).

Portland cement consists of OH, S-O, CO_3, Si-O and Al-O bonds (Gomes et al., 2005).

SO_4, caused by pollution, can transform into sulphuric acid. This conversion leads to the increased acidity of rain. Sulphuric acid can transform carbonates into calcium sulphate (gypsum ($CaSO_4.2H_2O$)) (Kootker, 2007a). Therefore, the presence of sulphate has nothing to do with the original composition.

Si-O bonds occur in clay and portland cement and can occur as small crushed quartz grains. Gypsum can occur because of pollution and in portland cement. Portland cement and a mixture of lime, which is partly transformed in gypsum, and clay can not be distinguished, since these mixtures both contain water, carbonoxide, sulphate, silicate and aluminiumoxides.

The presence of a C-H bond means that the sample contains organic matter. This can be charcoal, which could be added to the mortar, intentional or accidental during the heating. The formula of charcoal is C_7H_4O (Bretscher, 2009). It can also be recent organic material.

It is strange that Zc.6 contains brucite, but no silicates. Clay containing brucite should also contain silicates.

The fact that the samples which contain iron oxide are all in group 3, in which the Si-O band is smaller than the calcite band, does correspond with the results of the article of Genestar et al. (2006).

Comparison with site, building, date and building owner

The following groups were made based on the height of the calcite peak around 1420 cm^{-1} and the silicate peak around 1030 cm^{-1}:
Group 1: A.2.
Group 2: A.1, D.1, Zc.3, Zc.6 and Zc.8.
Group 3a: Vb.2, Vc.3, Vo.1.
Group 3b: Ba.2, Zc.7, Zc.9, Zc.10, Zw.1, Zw.2, Zw.4.
Group 3c: Ba.1, Ba.3, Bb.1, Bb.2, Bc.3, Bc.4, Bc.5, D.2, Va.1, Vb.1, Vc.1, Vc.2, Vd.1, Vn.1, Vs.1, W.1, W.3, W.4, W.5, W.6, Zc.1, Zc.2.
Group 4: Ba.4, Bc.1, Bc.2, Vg.1, Vw.1, W.2, Zc.4, Zc.5 and Zw.3.

A link between site or building and FT-IR results can only be seen at the samples of the church of Wulveringem, from which 5 out of 6 samples are in the same group, and at the wall of 'Hof te Zande', of which 3 out of 4 are in the same group.

The two samples of Aendijcke and the two samples of 'Ter Doest' are separated. The 11 samples of 'Ten Bogaerde' and the 12 samples from Veurne are divided among 3 groups. Most of these samples are in the largest group (3c). The 10 samples from the church of 'Hof te Zande'

are spread out over 4 groups.

A link between the date of the sample and the FT-IR group is only visible at the 18^{th} century barn of 'Ten Bogaerde'. The 2 samples from the northern side are in group 4, while the 3 samples from the southern side of the barn are in group 3c.

Furthermore, no link exists between the date of the sample and the FT-IR group. Group 1 contains only 1 sample, so nothing can be said about that. The samples in group 2 and 3b have dates between the 13^{th} and 20^{th} century, the buildings of group 3a have been dated $13/16^{th}$, 16^{th} and $17/18^{th}$ century, group 3c between the 12^{th} and 17^{th} century and group 4 between the 13^{th} and 18^{th} century.

The Cistercian buildings are scattered throughout the groups. The largest group (3c) shows ten samples from Cistercian buildings and twelve samples from other buildings, which is almost an equal amount. Group 4 contains six samples from Cistercian buildings and three samples from other buildings. The samples in group 3c are all from Cistercian buildings, but six out of seven samples are from 'Hof te Zande', so the location may have influenced this. Group 2 contains one sample from a non-Cistercian building and four samples from Cistercian buildings, of which three are from 'Hof te Zande'. The other two groups contain only one and three samples.

When looking to all components, it is noticed that the samples from Aendijcke do not contain iron oxide, sulphate and brucite. The samples from 'Ter Doest' do contain brucite, but no iron oxide and sulphate. This is an indication that the composition may be influenced by location, but this is not shown from the other samples.

W.6 differs from the other samples from Wulveringem in age, it is of a later building phase. Unlike at the other samples, the 1622 peak of W.6 is clearly visible in the spectrum. Some of the other Wulveringem samples only show a very small 1622 peak. This peak indicates sulphate, maybe gypsum. It is unlikely that the sulphate is caused by industrial pollution, since it is much more present in W.6 than in the other samples and the samples have been taken from the same location. It is possible that the sample is newer than expected and the sulphate originates from portland cement.

6.5 Comparing results from different methods

As macro-, microscopy, FT-IR and in a certain way TGA all measure composition, the results of these methods can be compared.

6.5.1 Macro- and microscopic results compared

The samples of microscopic group 1 (Zc.3 and Zc.7) are not in the same macroscopic groups based on colour and identifiable grains, neither are the samples of microscopic group 2a (W.4 and Zw.1). The samples of microscopic group 2b (Zc.1 and Zw.4) might be in the same group based on identifiable grains, but are not in the same group based on colour. Concluding, no resemblance can be seen between the macro- and microscopical groups.

Microscopy is more precise, so it is expected that during microscopy more aggregates could be found than during macroscopic examination. However, sometimes aggregates were found during macroscopy and not during microscopic analysis. This means that the sample was not very homogeneous. Sometimes, only one relatively large piece was found during macroscopic description, that has not ended up in the thin section.

Aggregates found during macroscopy, but not during microscopy:

A.1: brick	Zc.3:brick	Zc.7: lime, brick
A.2: shell	Zc.4: brick	Zw.1: shell
Bc.4: brick	Zc.6: lime	Zw.3: brick

After comparing the macro- and microscopic results, it was noticed that A.1 and A.2 contain the same aggregates, except for polycrystalline quartz.

Lime source

The lime in mortar could have been made of shells or limestone. Shells were found in the samples A.2, Bc.3, Bc.4 and Zw.1 using macroscopy and in the samples A.1, Bc.4, Vc.3, Zc.1 and Zw.4 using microscopy. However, these analyses did not show whether the lime was made of shells or limestone. Lime lumps and shells coexist in the samples, probably because the lime mixture was made first and the shells were added later. The shells are completely visible, while the lime lumps are burned.

While shells are visible in the lime, the lime could still have been made from limestone, since this can also contain shells. If limestone is not well heated when producing lime, a shell might remain in the mortar, but the structure may not be visible as well as in the studied samples. In addition, some limestone would probably be visible around the shell, but the shells in the studied samples are isolated aggregates.

Although the presence of shells does not prove them to be the source, it still is the most likely. Limestone can be found in the Belgium province Hainaut (Henegouwen), for example in Soignies (Zinnik) (F*édé*ration des Carrières de Petit Granit - Pierre Bleue de Belgique ASBL, 2006). This is just less than 100 km from the nearest locations (Kloosterzande and Aendijcke) and almost 130 km from Wulveringem, Veurne and 'Ten Bogaerde'. The area south-east of Gent contains calcareous sandstone and sandy limestone (Van der Kelen, 1996). The nearest sources are 40 km from Aendijcke to almost 80 km from 'Ten Bogaerde'. The samples locations are only 2 (Kloosterzande) (slightly further away when the church was build (de Kraker, 1997)) to 13 km (Wulveringem) from the coast, so it is much easier and cheaper to get shells from the coast than to obtain limestone.

6.5.2 FT-IR and TGA results compared

Table 6.1 clearly shows that most of the samples are in group 3 of the TGA results and in group 3c of the FT-IR results. This results in 16 of the samples being at both these groups.

Furthermore, the table shows a relation between the results of TGA and FT-IR. The samples which form a group based on the TGA results do not form the same groups based on the FT-IR results, but in general it can be said that whenever a sample is in a FT-IR group with a small number, it will not be in a TGA group with a large number and whenever a sample is in a TGA group with a large number, it will not be in a TGA group with a small number.

The TGA groups are based on the amounts of CO_2 and SBW, while the FT-IR groups are based on the amounts of calcite and silicates. The amount of calcite and CO_2 are related to each other. Silicates are a part of the hydraulic compounds, which the structurally bound water indicates. The fact that the TGA and FT-IR results do not form the same groups indicates that silicate is not the only hydraulic compound. Other compounds that influence the SBW could for example be organic material and iron oxide.

6.5.3 Macroscopic results compared to FT-IR and TGA results

The macroscopic results do not show a relation to the FT-IR and TGA results. Most samples are in FT-IR group 3c, TGA group 3, in the 10^{th} group of the macroscopic results based on colour, followed by the 8^{th} group, and in the 3^{rd} group of the macroscopic results based on

identifiable grains. Tables 6.2 and 6.3 show that the intersections of these groups give the highest amount of samples.

	FT-IR					
TGA	1	2	3a	3b	3c	4
1	1	1	1	1	1	1
2	0	0	0	2	1	2
3	0	4	2	3	16	1
4	0	0	0	1	3	1
5	0	0	0	0	0	4

Table 6.1: The amount of samples in groups based on FT-IR and TGA results.

		Macroscopy (colour)													
		1	2	3	4	5	6	7	8	9	10	11	12	13	14
FT-IR	NA	0	0	0	0	0	0	0	0	0	1	0	0	0	0
	1	0	0	0	0	0	0	1	0	0	0	0	0	0	0
	2	0	1	0	1	0	0/1	0	1	0	1/2	0	0	0	0
	3a	0	0	0	0	0	0	0	3	0	0	0	0	0	0
	3b	0	0	0	0	0	0	1	2	1	0	2	0	1	0
	3c	0	1	2	0	1	0	0	2	2	10	2	1	0	1
	4	1	0	0	0	0	0	0	0	1	5	1	0	0	1
TGA	NA	0	0	0	0	0	0	0	0	0	1	0	0	0	0
	1	0	1	0	0	1	0	1	3	0	1	0	0	0	0
	2	1	0	0	0	0	0	0	1	0	0	2	0	0	1
	3	0	1	1	1	0	0/1	1	4	1	11/12	3	1	1	
	4	0	0	1	0	0	0	0	0	3	1	0	0	0	0
	5	0	0	0	0	0	0	0	0	0	3	0	0	0	1

Table 6.2: The amount of samples in groups based on Macroscopy (colour), FT-IR and TGA results.

		Macroscopy (grains)												
		1	2	3	4	5	6	7	8	9	10	11	12	13
FT-IR	NA	0	0	0	0	1	0	0	0	0	0	0	0	0
	1	0	0	0	0	0	0	0	0	0	0	0/1	0	0/1
	2	0	1/2	2	0	0/1	0	0	0	0	0	1	0	0
	3a	1	0	0/1	0	0	0	0/1	0	0	0	1	0	0
	3b	1	0	3	0	0	2	0	0	1	0	0	0	0
	3c	4	0	7/8	1	0	2	1/2	2	1	1	0/1/2	0	0/1/2
	4	0	1	4/5	0	0	0/1	0/1	1	0	0/1	1	0	0
TGA	NA	0	0	0	0	1	0	0	0	0	0	0	0	0
	1	0	0	3/4	0	0	0	0/1	1	0	0	1/2	0	0/1
	2	1	1	2	0	0	1	0	0	0	0	0	0	0
	3	4	1/2	6/7	1	0/1	3	1/2	1	2	1	2/3/4	0	0/1/2
	4	1	0	4	0	0	0	0	0	0	0	0	0	0
	5	0	0	1/2	0	0	0/1	0/1	1	0	0/1	0	0	0

Table 6.3: The amount of samples in groups based on Macroscopy (identifiable grains), FT-IR and TGA results.

6.5.4 Microscopy results compared to FT-IR and TGA results

Microscopy does not show a relation to TGA and FT-IR. Table 6.4 shows that most samples are not measured with microscopy (not applicable: NA) or could not be grouped (no). The samples that could be grouped are mostly in TGA group 3, which is logical, since that is the largest group. And in FT-IR group 3b, but that are only 3 samples, only one more than in FT-IR group 3c, which is the largest group.

In addition, the binder/aggregate ratio estimated during microscopy and the amount of carbonate measured at TGA do not match. For example, the B/A ratio of Zc.6 is estimated

	TGA					FT-IR					
Microscopy	1	2	3	4	5	1	2	3a	3b	3c	4
NA	4	2	17	5	3	0	2	2	2	19	6
no	2	3	4	0	1	1	2	1	2	1	3
1	0	0	2	0	0	0	0	0	1	1	0
2	1	0	1	0	0	0	0	0	1	1	0
3	0	0	2	0	0	0	1	0	1	0	0

Table 6.4: The amount of samples in groups based on Microscopy, FT-IR and TGA results.

80/20, while the amount of carbonate measured with TGA is 33.48 wt.%. Of course the volume and weight don't match, but this is a very large difference.

6.6 Summary of the comparisons

The macroscopic results showed that a link between colour and the buildings may be present at the samples of 'Ter Doest' and 'Ten Bogaerde'. No clear relation was seen between the identifiable grains and the sites and buildings. No relation at all was seen between the colour of the samples and the initiator of the building, but some differences between the grain content and the initiators were seen. No clear relation could be seen between the date of the samples and the colour or grain content. Small differences that were observed could also have been influenced by the location.

The microscopy results show that groups can be made which are similar in site, date and building owner. However, a sample with a different location, date and building owner can also occur in the group, while a sample with the same location, date and building owner can not.

Using TGA, groups can be made of samples which correspond in site, especially at the samples from Aendijcke, 'Ter Doest' and 'Hof te Zande'. A link between the samples of a building is noticed at the samples of 'Hof te Zande' and the two barns from 'Ten Bogaerde'. TGA groups and date correspond only at the 18^{th} century barn of 'Ten Bogaerde'. No relation was found between the building owner and the TGA results.

A link between location and FT-IR groups could only be seen at 2 buildings, the church of Wulveringem and the wall of 'Hof te Zande'. The FT-IR peaks of the samples from Aendijcke show the same components, and the samples from 'Ter Doest' show the same peaks, but the peaks of these two locations differ in height. This shows that a link may exist between FT-IR results and location. FT-IR groups and date correspond at only one building, again at the 18th century barn of 'Ten Bogaerde'. The FT-IR peaks of W.6, which is of a later date, are slightly different from the other samples from the church of Wulveringem. No relation could be found between the building owner and the FT-IR results.

Except for a small difference between Cistercian and non-Cistercian buildings at the macroscopic groups based on identifiable grains, no link could be found between the building owner and the result. This can either mean that no relation is present, or that the relation between the results and the location is more dominant. The last may also be the case at the relation between the composition and the date. The samples with a different building owners always have and with a different date sometimes have a different location.

Table 6.5 gives an overview of all samples and in which group they are. It is strange that if groups are made, samples of the same location, building and building owners are not necessarily in the same groups, as Zc.4 and Zc.6, and samples from different locations, dates and owners are sometimes in the same groups, for example W.3 and Zc.2. The last occurs often, especially at samples which are in the largest groups (group 10 at macroscopy based on colour, group 3 at macroscopy based on identifiable grains, group 3 at TGA and group 3c at FT-IR).

Sample	Century	Macroscopy (colour)	Macroscopy (grains)	Microscopy	TGA	FT-IR
A.1	$\leq 16^{th}$h	10	2/5	no	3	2
A.2	$\leq 16^{th}$	7	11/13	no	1	1
Ba.1	13^{th}	9	11/13		3	3 c
Ba.2	13^{th}	9	3		4	3 b
Ba.3	13^{th}	9	3		4	3 c
Ba.4	13^{th}	14	3		5	4
Bb.1	17^{th}	10	11/13		3	3 c
Bb.2	17^{th}	10	10		3	3 c
Bb.3	17^{th}	10	5			
Bc.1	18^{th}	10	6/10		5	4
Bc.2	18^{th}	10	3/7		5	4
Bc.3	17^{th}	10	9		3	3 c
Bc.4	17^{th}	12	6	no	3	3 c
Bc.5	17^{th}	10	3		4	3 c
D.1	$13/14^{th}$	2	3		1	2
D.2	$13/14^{th}$	2	6		3	3 c
Va.1	$15/17^{th}$	14	3		2	3 c
Vb.1	$13/16^{th}$	8	8		1	3 c
Vb.2	$13/16^{th}$	8	11		3	3 a
Vc.1	16^{th}	10	1		3	3 c
Vc.2	16^{th}	10	4		3	3 c
Vc.3	16^{th}	8	1	no	3	3 a
Vd.1	13^{th}	3	7		3	3 c
Vg.1	$16/17^{th}$	10	8	no	5	4
Vn.1	13^{th}	10	1		3	3 c
Vo.1	$17/18^{th}$	8	3/7		1	3 a
Vs.1	15^{th}	3	1		4	3 c
Vw.1	13^{th}	9	3		4	4
W.1	12^{th}	11	3		3	3 c
W.2	12^{th}	10	3		3	4
W.3	12^{th}	10	3		3	3 c
W.4	12^{th}	8	8	2a	3	3 c
W.5	12^{th}	5	3		1	3 c
W.6	16^{th}	10	1		3	3 c
Zc.1	13^{th}	11	3/7	2b	3	3 c
Zc.2	13^{th}	10	3		3	3 c
Zc.3	20^{th}	6/10	2	1	3	2
Zc.4	13^{th}	1	2	no	2	4
Zc.5	13^{th}	11	3		2	4
Zc.6	13^{th}	8	3	no	3	2
Zc.7	20^{th}	13	6	1	3	3 b
Zc.8	17^{th}	4	11		3	2
Zc.9	17^{th}	7	3		3	3 b
Zc.10	17^{th}	11	6	2	2	3 b
Zw.1	$\geq 17^{th}$	11	9	2a	3	3 b
Zw.2	$\geq 17^{th}$	8	1	2	2	3 b
Zw.3	$\geq 17^{th}$	10	11	2	1	4
Zw.4	$\geq 13^{th}$	8	3	2b	1	3 b

Table 6.5: Group comparison

Chapter 7

Conclusion and outlook

The aim of this thesis has been to discover whether the location, date and initiators of the buildings (Cistercian or non-Cistercian) had influence on the composition of the mortar.

Therefore, the following questions needed to be answered:

- *Do mortars show differences in terms of location, period and owner of the building?*
  - *What is the composition of the sampled mortars?*
    - *What is the provenance of the material? Does the lime from the mortar come from shells or from limestone?*
  - *What groups of building styles can be made based on the composition of these samples?*

The composition of the mortars is presented by the macro-, microscopic, TGA and FT-IR results. The mortars mostly contained lime, but also silicates, organic material, charcoal, iron oxides, clay, shells etc. were present.

The results of the microscopic analysis show that all quartz grains, except for the modern ones, are angular, so they come from rivers. This rejects the hypothesis made in chapter 2, which was that the quartz sand which was used came from the beach. The analyses did not provide evidence of shells being the lime source, but regarding distance, this is the most logical source.

The groups which were made based on the results of the different methods do not correspond, so building styles could not be distinguished based on the composition.

Since no link exists between the results and the date, possible samples with an unknown date could not be dated. However, a difference between older and newer material was noticed at the 18^{th} century barn at 'Ten Bogaerde' using TGA and FT-IR.

Groups based on TGA results correspond in location, while groups made of microscopy and FT-IR results only partially relate.

No relation could be found between the results and the building owner, except for a small difference at the macroscopic groups based on identifiable grains.

The above shows that the groups based on the results from the various methods correspond the most to location, so it can be concluded that local material was used to make mortar. This is consistent with the hypothesis.

Analysing mortars from more buildings will improve the result, since if mortars from different centuries and building owners are taken from every location, it will be easier to prove whether the composition is influenced by the location, date or building owner. Samples of consolidated material are needed in order to make additional thin sections. An architectural historian has to study the to be sampled buildings to distinguish different building phases.

In addition, a historian can study literature to see whether methods to produce lime mortar which have been described in the past correspond to the composition of mortar in this study and to the results that local material was used.

It is not yet known whether the result, that local material was used for producing mortar, can also be applied to other regions. A challenge for future research is to test this.

Acknowledgements

I would like to thank all the people who helped me with this thesis.

First of all, Henk Kars and Adriaan de Kraker for supervising me in writing this thesis. Henk Kars also for giving advice how to interpret the thin sections. Adriaan de Kraker and his wife Nellie for their hospitality to let me stay over for two nights during my fieldwork in Kloosterzande. I want to thank Dave van der Brugge for lending me his car for fieldwork and Debbie van Balen-Trevor for answering my questions about English grammar. I appreciate the help of Lisette Kootker, who explained her own research and advised me on how I could best do my research,

I would like to express my gratitude to all the people who helped me obtaining my samples. Pieter Overduin, Cor Crans (foundation 'De Kerk in Klooster') and the church of Kloosterzande for letting me sample their church and explaining history of the church. Vincent Debonne, researcher of architectural heritage, for information about the building phases of the church of Kloosterzande. Harry van Royen of the Abbey Museum 'Ten Duinen 1138' in Koksijde for guiding me to the research that took place in Belgium and helping me obtaining information. Alexander Lehouck for a guided tour at 'Ten Bogaerde', the city Veurne and the church at Wulveringem, and for providing samples of his own research for me to analyse. Director of the school 'School van de Vlaamse Gemeenschap' in Veurne Martin Boudry for allowing me to sample the school. And Benoit Delaey for a guided tour at Ter Doest.

Facilities for microscopical, TGA and FT-IR analyses were provided by the Vrije Universiteit Amsterdam. I would like to thank all the people who helped me with the analyses. Roel van Elsas of the mineral separation laboratory for providing instruments for sieving the samples. Wynanda Koot and others of the Geological Technical Laboratory of the VU for making thin sections. Saskia Kars who showed me how the camera of the microscope worked. Freek Ariese (of the chemistry department of the VU) for explaining both methods of FT-IR (ATR and KBr). Hege Hollund for explaining ATR-FTIR and doing some test measurements with me. Elwin Janssen (of the organic chemistry department at the VU) of the ATR-FTIR, for allowing me to do test ATR-FTIR measurements. And Martin Konert for helping with the TGA analysis.

Finally, I would like to thank my family and friends, especially my parents and Dave, for supporting me in writing this thesis.

References

Bibliography

Ariese, F. and I. Petterson (2010). *Basispracticum Scheikunde 2010 - Instrumentele Analyse - Spectroscopische Technieken.*

Bakolas, A., G. Biscontin, A. Moropoulou, and E. Zendri (1995). Characterization of the Lumps in the Mortars of Historic Masonry. *Thermochimica Acta*, 809-816.

Bakolas, A., G. Biscontin, A. Moropoulou, and E. Zendri (1998). Characterization of Structural Byzantine Mortars by Thermogravimetric Analysis. *Thermochimica Acta 321*, 151-160.

Balen, K. van (2003). *Kalkboek: het gebruik van Kalk als Bindmiddel voor Metsel- en Voegmortels in Verleden en Heden.* Rijksdienst van de Monumentenzorg, Zeist.

Barclay Lloyd, J. (2006). *Ss. Vincenzo e Anastasio at Tre Fontane near Rome: history and architecture of a medieval Cistercian abbey.* Cistercian Publications, Collegeville.

Bleeckere, S. de (2005). Het tijdperk van het monachisme. In D. Vanclooster (Ed.), *De Duinenabdij van Koksijde, Cisterciënzers in de Lage Landen*, 12-23. Lannoo, Tielt.

Biscontin, G. (2002). Characterization of Binders Employed in the Manufacture of Venetian Historical Mortars. *Journal of Cultural Heritage 3*(1), 31-37.

Chorley, R. J., S. A. Schumm, and D. E. Sugden (1985). *Geomorphology.* Methuen Co., New York.

Delaey, B. (2005). De Cisterciënzer Abdijarchitectuur. In D. Vanclooster (Ed.), *De Duinenabdij van Koksijde, Cisterciënzers in de Lage Landen*, 119-146. Lannoo, Tielt.

Delaey, B. (2008). Geprofileerde Bakstenen in de Schuur van Ter Doest in Lissewege. *Novi Monasterii 7*, 293-298.

Devliegher, L. (1954). *De opkomst van de kerkelijke gotische bouwkunst in West-Vlaanderen gedurende de XIIIe eeuw.* Genootschap voor Geschiedenis, Brugge.

Dewilde, M. and J. D. Meulemeester (2005). Archeologie, Geschiedenis en Bouwhistorie. In D. Vanclooster (Ed.), *De Duinenabdij van Koksijde, Cisterciënzers in de Lage Landen*, 180-195. Lannoo, Tielt.

Durbin, L. (2005). *Architectural Tiles: Conservation and Restoration : from the Medieval Period to the Twentieth Century.* Butterworth-Heinemann, Oxford.

Elsen, J. (2006). Microscopy of Historic Mortars - a Review. *Cement and Concrete Research 36*, 1416-1424.

Faure, G. (1998). *Principles and Applications of Geochemistry.* Prentice Hall, New Jersey.

Firmin (De Smidt), B. (1940). *De Romaansche Kerkelijke Bouwkunst in West-Vlaanderen.* Universitaire Stichting van België, Brussel.

Fruytier, A. (1950). *Geschiedenis van Hontenisse.* Bornem/Hontenise.

Genestar, C. and C. Pons (2005). Earth Pigments in Painting: Characterisation and Differentiation by means of FTIR Spectroscopy and SEM-EDS Microanalysis. *Analytical and Bioanalytical Chemisty 382*(2), 269-274.

Genestar, C., C. Pons, and A. Más (2006). Analytical Characterisation of Ancient Mortars from the Archaeological Roman City of Pollentia (Balearic Islands, Spain). *Analytica Chimica Acta, 557*(1-2), 373-379.

Gleize, P. J. P., E. V. Motta, D. A. Silva, and H. R. Roman (2009). Characterization of Historical Mortars from Santa Catarina (Brazil). *Cement and Concrete Composites 31*(5), 342-346.

Gomes, C. E. M., O. P. Ferreira, and M. R. Fernandes (2005). Influence of Vinyl Acetate-Versatic Vinylester Copolymer on the Microstructural Characteristics of Cement Pastes. *Materials Research 8*(1), 51-56.

Kinder, T. N. (2002). *Cistercian Europe: Architecture of Contemplation.* Wm. B. Eerdmans Publishing, Grand Rapids.

Kootker, L. M. (2007a). *The Roman Theatre in Ancient Nikopolis, Epirus, Greece.*

Kootker, L. M. (2007b). *On the Binder of Mortars from Nikopolis, Greece.*

Kraker, A. M. J. de (1997). *Landschap uit Balans: de Invloed van de Natuur, de Economie en de Politiek op de Ontwikkeling van het Landschap van de Vier Ambachten en het Land van Saeftinghe tussen 1488 en 1609.* Matrijs, Utrecht.

Kreh, R. T. (2002). *Masonry Skills.* Cengage Learning, Clifton Park.

Kristof, J., J. Mink, E. Horvath, and M. Gábor (1993). Intercalation Study of Clay Minerals by Fourier Transform Infrared Spectrometry. *Vibrational Spectroscopy 5*, 61-67.

Lehouck, A. (2001). *Onder de Deklaag: Archeologische Bijdrage tot de Ontwikkeling Historische Topografie van Middeleeuws Veurne.*

Lehouck, A. (2002). Bouwhistorisch Onderzoek in de Noordstraat te Veurne (W.-Vl.). *Archaeologia Mediaevalis 25*, 67-69.

Lehouck, A. (2008). Gebruik en Productie van Baksteen in de Regio Veurne van circa 1200 tot circa 1550. *Novi Monasterii 7*, pp. 203-232.

Lehouck, A. (2010). *Abdijhoeve Ten Bogaerde (gem. Koksijde). Bouwhistorisch Onderzoek van de Varkensstallen.* Technical report.

Leysen, L. A., E. J. Roekens, R. E. van Grieken, and G. de Geyter (1990). Characterization of the Weathering Crust of Various Historical Buildings in Belgium. *The Science of the Total Environment 90*, 117-147.

Maravelaki-Kalaitzaki, P., A. Bakolas, A. Moropoulou (2003). Physico-Chemical Study of Cretan Ancient Mortars. *Cement and Concrete Research 33*, 651-661.

Mcbride, E. F. and M. Dane Picard (1987). Downstream Changes in Sand Composition, Roundness, and Gravel Size in a Short-headed, High-Gradient Stream, Northwestern Italy. *Journal of Sedimentary Petrology Vol. 57*(6), 1018-1026.

Mertens, G., J. Elsen, R. Brulet, A. Brutsaert and M. Deckers (2009). Quantitative Composition of Ancient Mortars from the Notre Dame Cathedral in Tournai (Belgium). *Materials Characterization 60*, 580-585.

Moffett, M., M. W. Fazio and L. Wodehouse (2003). *A World History of Architecture.* Laurence King Publishing Ltd, London.

Moropoulou, A., A. Bakolas, and K. Bisbikou (2000). Investigation of the Technology of Historic Mortars. *Journal of Cultural Heritage 1*, 45-58.

Moropoulou, A., K. Polikreti, A. Bakolas, and P. Michailidis (2003). Correlation of Physicochemical and Mechanical Properties of Historical Mortars and Classification by Multivariate Statistics. *Cement and Concrete Research 33*, 891-898.

Nichols, G. (2009). *Sedimentology and Stratigraphy.* Blackwell Science Ltd., Malden.

Pavia, S., and S. Caro (2008). An Investigation of Roman Mortar Technology through the Petrographic Analysis of Archaeological Material. *Construction and Building Materials 22*, 1807-1811.

Pettijohn, F. J., P. E. Potter, and R. Siever (1987). *Sand and Sandstone.* Springer-Verlag, New York.

Provoost, T. (1997). De IJzer: een Kleine Stroom met een Groot Verleden. *Water 97*, 233-238.

Rampazzi, L. and R. Bugini (2006). St. Lorenzo Basilica in Milan: Integral Approach of Characterisation of Historical Mortars. *E-Preservation Science*, 21-26.

Regev, L., K. M. Poduska, L. Addadi, S. Weiner, and E. Boaretto (2010). Distinguishing between Calcites formed by different Mechanisms using Infrared Spectrometry: Archaeological Applications. *Journal of Archaeological Science 37*, 3022-3029.

Royen, H. van (2005). Het Monastieke Leven van de Broeders van Ten Duinen, 1107-1833. In D. Vanclooster (Ed.), *De Duinenabdij van Koksijde, Cisterciënzers in de Lage Landen*, 61-86. Lannoo, Tielt.

SCEZ (Stichting Cultureel Erfgoed Zeeland) (2010). Cisterciënzer Baksteengotiek in Kloosterzande. *Zeeuws Erfgoed 2*, 11.

Silva, D. A., H. R. Wenk, and P. J. M. Monteiro (2005). Comparative Investigation of Mortars from Roman Colosseum and Cistern. *Thermochimica Acta 438*(1-2), 35-40.

Socrates, G. (2004). *Infrared and Raman Characterisic Group Frequencies: Tables and Charts.* John Wiley and Sons Ltd., Chichester.

Stichting de Kerk in Klooster (2009). *De Hof te Zande Kerk, 1209-2009. Een Kleine Geschiedenis.*

Terry, R. and G. Chilingar (1955). Summary of 'Concerning some Additional Aids in Studying Sedimentary Formations' by M. S. Shvetsov. *Journal of Sedimentary Research 25*, 229-234.

Twenhofel, W. H. (1945). The Rounding of Sand Grains. *Journal of Sedimentary Petrology 15*(2), 59-71.

Vanderputten, S. (2005). Moeders en dochters. In D. Vanclooster (Ed.), *De Duinenabdij van Koksijde, Cisterciënzers in de Lage Landen*, 46-59. Lannoo, Tielt.

Velosa, A., J. Coroado, M. R. Veiga, and F. Rocha (2007). Characterisation of Roman Mortars from Conimbriga with Respect to their Repair. *Materials Characterization 58*(11-12), 1208-1216.

Wenk, H.-R. and A. G. Bulakh (2004). *Minerals: their Constitution and Origin.* Cambridge University Press, Cambridge.

Whittaker, D. (2000). *Interpreting Organic Spectra.* Royal Society of Chemistry, Cambridge.

Websites

Bretscher, U. (2009). *Charcoal.* `http://www.musketeer.ch/blackpowder/charcoal.html`

Fédération des Carrières de Petit Granit - Pierre Bleue de Belgique, ASBL (2006). *Natuur en oorsprong van Arduin - Belgische blauwe hardsteen.* `http://www.federationpierrebleue.be/natuur.htm`

Google Earth (2010). `http://earth.google.com`

Google Maps (2010). `http://maps.google.com`

International Scheldt Commission (2011). *The Scheldt at a Glance.* `http://www.isc-cie.org/en/the-scheldt-at-a-glance.html`

Kelen, I. van der (1996). *Steengroeven te Houtem.* `http://www.freewebs.com/darcos/Steengroeven%20te%20Houtem.pdf`